

# Advances in 3D Neural Stylization: A Survey

Yingshu Chen<sup>1</sup>, Guocheng Shao<sup>1</sup>, Ka Chun Shum<sup>1</sup>, Binh-Son Hua<sup>2</sup>, Sai-Kit Yeung<sup>1</sup>

<sup>1</sup>The Hong Kong University of Science and Technology <sup>2</sup>Trinity College Dublin

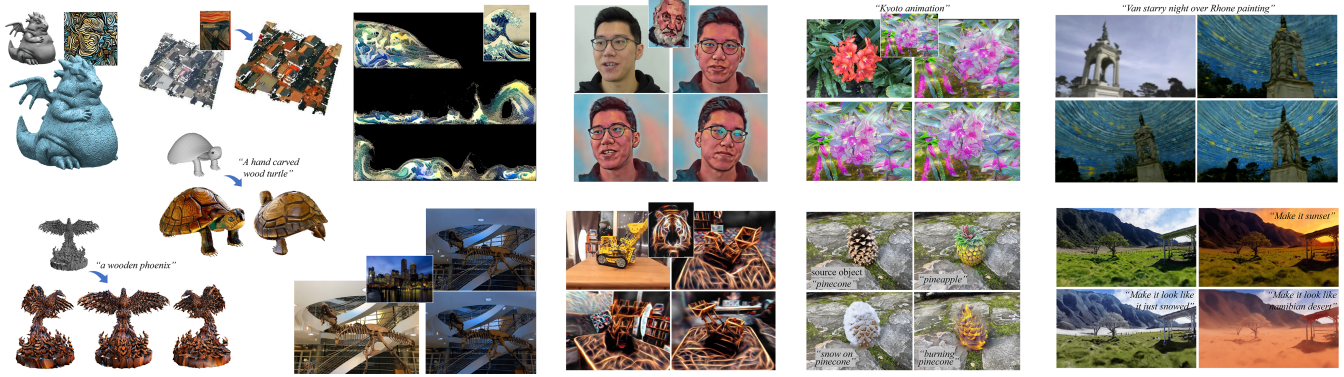


Figure 1: The state-of-the-art report delves into the realm of neural stylization on diverse 3D representations, including meshes, point clouds, volumetric simulation, and implicit fields. The capabilities of image-guided and text-guided neural stylization empower artistic, photorealistic, and semantic style transformation of the geometry and/or appearance of 3D scenes. Images adapted from [LTJ18, MZS\*23, CWNN20, RMA\*23, WCF\*23, ZKB\*22, ZHX\*23, SCD\*23, WCF\*23, HTE\*23].

## Abstract

Modern artificial intelligence provides a novel way of producing digital art in styles. The expressive power of neural networks enables the realm of visual style transfer methods, which can be used to edit images, videos, and 3D data to make them more artistic and diverse. This paper reports on recent advances in neural stylization for 3D data. We provide a taxonomy for neural stylization by considering several important design choices, including scene representation, guidance data, optimization strategies, and output styles. Building on such taxonomy, our survey first revisits the background of neural stylization on 2D images, and then provides in-depth discussions on recent neural stylization methods for 3D data, where we also provide a mini-benchmark on artistic stylization methods. Based on the insights gained from the survey, we then discuss open challenges, future research, and potential applications and impacts of neural stylization.

## CCS Concepts

• *General and reference* → *Surveys and overviews*; • *Computing methodologies* → *Rendering*; *Computer vision representations*;

## 1. Introduction

Digital art and visual design have been prevailing in our daily life spaces, expressing visually captivating aesthetics, unique tastes, and emotions of human beings. With the recent advancements in computing hardware, creating high-quality arts digitally with computational tools or algorithms receives increasing public attention. The appearance of artificial intelligence (AI) techniques further boost this computational design process and show strong potential to accelerate or automate the creation of digital arts. Emerging visual synthesis and editing AI products such as LUMA AI [Lum23], DALL·E 3 [Ope23], Midjourney [Mid23], and RunwayML [Run23]

have successfully demonstrated their ability to speed up the high-quality visual design and generation.

This report delves into recent advances in AI for creating 3D digital arts through stylization. A typical stylization of a 3D scene involves editing the scene geometry and/or the appearance to match some specified artistic styles. Stylization can be achieved with a neural network in modern deep learning, hence the term neural stylization. Putting into the context of a traditional computer graphics pipeline, 3D neural stylization can be regarded as an alternative to the custom rendering pipeline with programmable shaders used for stylization as post-processing. Therefore, 3D neural stylization

helps reduce the labor-intensive manual work in styling a 3D scene including 3D modeling, texturing, rendering, or simulation. 3D neural stylization thus has practical values for various industrial applications, including 3D texture design and artistic simulation in movie making [NR21, KAOT23, HHK\*23], mixed reality experiences [THC\*22, Tan19] (Figure 2), photorealistic visual effects (VFX) and virtual production [Man23], artwork creation [GC22] and video game development [OBW22, MLS\*22].

Extended from 2D neural stylization, 3D neural stylization performed using traditional 3D representations and rendering is usually confronted with view consistency and photorealistic rendering issues. Thanks to advances in neural rendering techniques, there has been significant improvement in 3D neural stylization with high-quality results for different 3D representations including mesh, volume, point cloud, and neural fields. It is also applicable for various 3D scenarios ranging from small object-only scenes to large in-the-wild scenes, and even applied to industrial production [HHK\*23].

In this report, we cover the stylization fundamentals, recent advances, existing challenges, and future research directions in the field of 3D neural stylization. We begin with a review of fundamental techniques of neural stylization (Section 2) including 2D visual style transfer algorithms and 3D neural rendering. In Section 3, we introduce a taxonomy for neural stylization and provide a categorization for the state of the art in 3D neural stylization. Using this taxonomy, we discuss advanced 3D neural stylization methods in depth and put forward our analysis of the recent difficulties in 3D stylization. In Section 4, we summarize the frequently used datasets for 3D stylization evaluation. We also deliver a mini-benchmark to serve as a standard for performance evaluations of the state of the art 3D stylization algorithms. Finally, we discuss open challenges and future research direction in Section 5. We will release our evaluation codes and other implementation resources with the report.

### 1.1. Scope of this Report

The scope of this report focuses on neural style transfer specifically applied to 3D scenes. The objective is to explore deep learning based techniques and methodologies that enable the automated transfer of artistic or photorealistic styles and semantic characteristics to the 3D digital world. While acknowledging the scarcity and challenges of dedicated 3D training datasets for stylization, this report aims to highlight the potential of image-guided and text-guided neural stylization powered by off-the-shelf large data models to achieve visually appealing 3D stylized results.

## 2. Fundamentals on Neural Stylization

Visual style transfer refers to the task of editing the texture or color of a scene to match the style defined by a reference, while keeping the overall scene structure intact. In this section, we first provide an overview of 2D neural stylization as fundamentals. We focus on image-guided and text-guided style transfers as they are the two main sources of stylization methods that indicates a target style reference by an image or a piece of text, respectively. We start our discussion about the fundamentals with the simple methods that use classic feature extractors such as VGG classifiers and CLIP encoders. We also categorize these 2D neural style transfer techniques

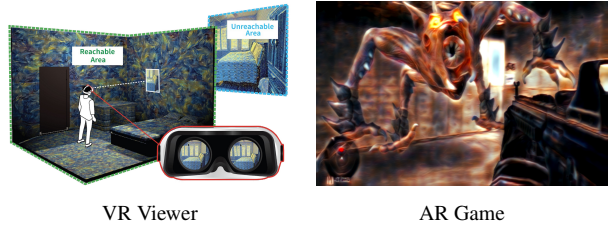


Figure 2: VR and AR applications with neural stylization. Left: Stylized VR scene touring with stylized novel views. Right: Real-time AR game with the virtual monster in stylized rendering. Images from Tseng *et al.* [THC\*22], Taniguchi [Tan19].

based on their optimization approaches. Last, we briefly introduce the basics of neural radiance fields, an important type of 3D neural representation, before deeper discussion about 3D neural stylization in Section 3. We refer to the surveys of [JYF\*19, SJJ\*21, ZYW\*23] for more discussion on conditional image synthesis and stylization, and [TTM\*22, XTS\*22] for more discussion on scene representations and neural rendering.

### 2.1. A Classic 2D Visual Style Transfer Algorithm

We begin with the most basic neural style transfer algorithm that optimizes a single image with a single style reference supervised by neural features. Gatys *et al.* [GEB16] observed that a deep convolutional neural network (CNN) can extract both appearance and style features of arbitrary images, and introduced a novel neural style transfer approach by optimizing an output image (see Figure 3). They sought to preserve the general appearance of the input source image by penalizing the differences in low-frequency (or high-level) spatial content features, while simultaneously infusing the style of the reference image into output by matching the feature correlation summary statistics. They propose the content and style losses based on latent features extracted from a pre-trained CNN model, specifically employing the VGG-19 network [SZ15] trained on the ImageNet dataset [DDS\*09]. Mathematically, given a content source image  $c$  and a style reference image  $s$ , the aim is to optimize a white noise image into an output stylized image  $cs$  with the content of the source image and the style of the reference image. We minimize the following objective function:

$$\mathcal{L}_{total}(c, s, cs) = \mathcal{L}_c(c, cs) + \lambda \mathcal{L}_s(s, cs), \quad (1)$$

where  $\mathcal{L}_{total}$  is the total loss comprised of a content loss  $\mathcal{L}_c$  between source image and stylized image, and a style loss  $\mathcal{L}_s$  between reference image and stylized image.  $\lambda$  is a hyperparameter that represents the weights between content and style losses. The **content loss** is defined as a squared-error loss between the two feature representations of source image  $c$  and stylized image  $cs$ :

$$\mathcal{L}_c(c, cs) = \sum_{l \in l_c} \|F^l(c) - F^l(cs)\|_2^2, \quad (2)$$

where  $F^l(\cdot)$  is the embedded feature representation of input image from layer  $l$  in VGG. Style information is represented by the Gram matrix of latent features, which indicates feature correlations and

forms a style feature space of an image. The **style loss** is defined as:

$$\mathcal{L}_s(s, cs) = \sum_{l \in l_s} \frac{1}{H^l W^l} \sum_{i,j} \|G^l(F^l(s))_{ij} - G^l(F^l(cs))_{ij}\|_2^2, \quad (3)$$

where  $G(F^l(\cdot)) = [F^l(\cdot)][F^l(\cdot)]^T$  is the Gram matrix of the feature map  $F^l(\cdot) \in \mathbb{R}^{H^l \times W^l \times d}$ ,  $l_c$  is a set of high layers in VGG used for content loss and  $l_s$  is a set of layers in VGG used for style loss. Note that the discussed losses have minor difference from the original paper as we assume all features and Gram matrices are normalized. Also,  $l_c$  usually contains only one layer such as *relu4\_1*, *relu4\_2* (used in [GEB16]), or *relu5\_1*.  $l_s = \{relu1_1, relu2_1, relu3_1, relu4_1, relu5_1\}$  is used in [GEB16].

The proposed content and style losses have a far-reaching impact on visual style transfer applications. Subsequent works [JAFF16, HB17, WLV21] adopt the same or similar loss strategies for neural stylization. The underlying principle shared by these works is to extract implicit content and style representations from a pre-trained network, and optimize the stylization performance of the output according to the content and style losses. VGG remains most widely used in neural style transfer, while other CNNs such as GoogleNet [SLJ\*15], ResNet [HZRS16] are possible for stylization [MOT15, WLV21].

### 2.1.1. Text-guided optimization

Recently, the rise of large-language models (LLMs) and their applications to visual computing has enabled a new form of style transfer guided by text prompts [PWS\*21, GPM\*22, KY22, KKY22, YHY23]. A typical approach is to use CLIP [RKH\*21], a pre-trained network that allows semantic similarity evaluation between text-image embedding given by a pretrained text encoder and a pretrained image encoder. A **CLIP loss**  $\mathcal{L}_{clip}$  can be used to guide the visual style transfer:

$$\mathcal{L}_{clip}(s, cs) = 1 - \text{CosSim}(E_I(cs), E_T(s)), \quad (4)$$

where  $cs$  and  $s$  are the output image and style text prompt.  $E_I$  and  $E_T$  are the pre-trained CLIP image encoder and text encoder, respectively.  $\text{CosSim}(A, B) = \frac{A \cdot B}{\|A\| \|B\|}$  is the cosine similarity between two feature vectors.

To realize better style transfer, [PWS\*21, GPM\*22] used **directional CLIP loss**  $\mathcal{L}_{dir}$  for image optimization:

$$\begin{aligned} \mathcal{L}_{dir}(c, cs, s_{src}, s_{sty}) &= 1 - \text{CosSim}(\Delta I, \Delta T), \\ \Delta I &= E_I(cs) - E_I(c), \\ \Delta T &= E_T(s_{sty}) - E_T(s_{src}), \end{aligned} \quad (5)$$

where  $c$  is the content image,  $cs$  is the stylized image,  $s_{src}$  and  $s_{sty}$  are source (content) style prompt and target style prompt. An example of  $s_{src}$  and  $s_{sty}$  can be “Photo” and “Picasso style painting”, respectively [KY22]. Since CLIP does not support high-resolution image embedding, Kwon *et al.* [KY22] introduced patch-wise directional CLIP loss with augmented patches for better artistic semantic texture transfer. Specifically, they proposed to randomly sample patches of the output image and augment patches with random transformation for CLIP directional loss. More recently, researchers tend to investigate the contrastive learning [PEZZ20] and diffusion

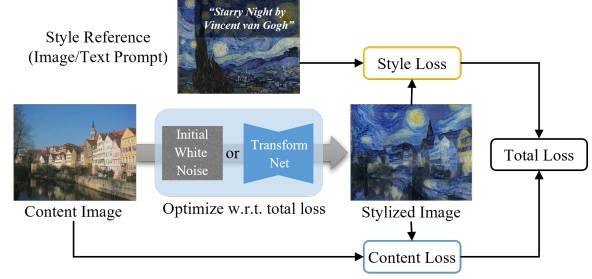


Figure 3: General 2D neural style transfer optimization framework [GEB16, JAFF16, KY22].

model [RBL\*22] for more accurate and higher-fidelity text-guided stylization [YHY23].

## 2.2. Advanced 2D Visual Style Transfer

While the classic visual style transfer algorithm achieves high-quality stylization results, there remains some practicality concerns to address. First, its output is obtained via an optimization that can take a few minutes to complete. Additionally, the classic algorithm only supports a single style, which means that to change to a new style, the optimization has to be started from scratch. Let us now explore more advanced visual style transfer algorithms that aim at addressing such limitations.

### 2.2.1. Multiple Style Transfer

To perform style transfer in real time, Johnson *et al.* [JAFF16] used a feedforward transformation network trained with a perceptual loss. At inference, the stylization can be done by simply forwarding the input image through the network. As shown in Figure 3, the transformation network is trained to minimize the content and style losses (Eq. 2, 3) using stochastic gradient descent. The network was trained with the large-scale MS-COCO dataset [LMB\*14]. Their method, however, binds a single style to each network, which means that a new network must be trained for each different style.

Subsequent real-time style transfer methods aim to support multiple styles in a single network by establishing conditional style transfers for several target styles. Dumoulin *et al.* [DSK17] extended instance normalization (IN) [UVL16] technique to condition style index, and proposed conditional instance normalization (CIN), defined as  $CIN(F(c), s_i) = \gamma_i \left( \frac{F(c) - \mu}{\sigma} \right) + \beta_i$ , where  $\mu$  and  $\sigma$  are mean and standard deviation of  $F(c)$  across  $c$ 's spatial dimensions (i.e., the number of batches and channels);  $\gamma_i$  and  $\beta_i$  are obtained by selecting the row corresponding to  $s_i$  in matrices  $\gamma$  and  $\beta$ , which represent the style's corresponding scaling and shifting parameters to be fine-tuned. With CIN, style of the stylized image can vary by interpolating  $\gamma$  and  $\beta$  between different target style images, thus achieving style interpolation. A trained model learns only a small set of *multiple styles* for stylization.

### 2.2.2. Arbitrary Style Transfer

A family of visual style transfer methods aim to support stylization with an arbitrary style. This can be achieved with data-driven image-to-image (I2I) translation networks. We briefly introduce feature



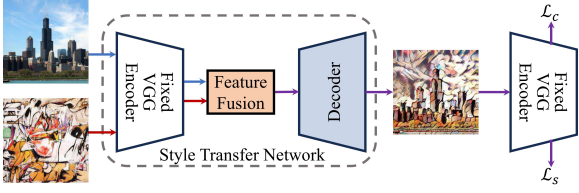


Figure 4: Overview of arbitrary style transfer algorithm. VGG encoder is pre-trained and fixed during network training. Feature fusion module can be such as AdaIN [HB17], transformation network [LLKY19].

normalization and learnable feature transformation techniques for arbitrary style transfer models in this section, and then mention popular generative models (i.e., GAN and diffusion model) for I2I problem in the next section. We refer readers to [ZYW\*23] for a detailed discussion of generative models.

**Feature Normalization and Fusion.** Previously mentioned real-time visual style transfer methods (Section 2.2.1) enables stylization with seen styles only. To achieve universal style transfer, Huang and Belongie introduced **adaptive instance normalization (AdaIN)** [HB17]. The key idea of AdaIN is that the stylized image can be controlled by its feature statistics. Unlike CIN [DSK17], AdaIN has no learnable scaling or shifting (a.k.a, affine) parameters. Instead, AdaIN tries to match channel-wise mean and variance feature statistics between content and style feature maps from encoder:

$$AdaIN(c, s) = \sigma(F(s)) \left( \frac{F(c) - \mu(F(c))}{\sigma(F(c))} \right) + \mu(F(s)), \quad (6)$$

where  $F(c)$  and  $F(s)$  are feature maps of the content image  $c$  and style image  $s$  extracted from the pre-trained VGG encoder, particularly  $F(\cdot) = F^{relu4\_1}(\cdot)$  in use;  $\mu(\cdot)$  and  $\sigma(\cdot)$  are channel-wise mean and standard deviation of the feature map.

The overview of the whole arbitrary style transfer network is illustrated in Figure 4. VGG encoder  $F$  is composed of first few layers (up to  $relu4\_1$ ) of a pretrained VGG. The style transfer network  $\mathcal{N}(c, s)$  follows encoder-decoder architecture, and fix the encoder during training. VGG encoder encodes input source content  $c$  and style  $s$  images to latent feature space, and feeds both feature maps ( $F(c)$  and  $F(s)$ ) to an AdaIN layer (Eq. 6). AdaIN regulates mean and variance of the content feature maps to match those of style feature maps, and feeds new stylized feature maps  $t = AdaIN(c, s)$  into decoder  $G$ . A randomly initialized decoder  $G$  is trained to map latent feature  $t$  back to the image space, generating the stylized image  $cs = G(t)$ . The network is trained with weighted content loss  $\mathcal{L}_c$  and style loss  $\mathcal{L}_s$  as follows:

$$\begin{aligned} \mathcal{L}_{total} &= \mathcal{L}_c(c, cs) + \lambda \mathcal{L}_s(s, cs), \\ \mathcal{L}_c(c, cs) &= \|t - F(cs)\|_2, \\ \mathcal{L}_s(s, cs) &= \sum_{l \in l_s} \|\mu(F^l(s)) - \mu(F^l(cs))\|_2 \\ &\quad + \sum_{l \in l_s} \|\sigma(F^l(s)) - \sigma(F^l(cs))\|_2, \end{aligned} \quad (7)$$

where  $\lambda$  is the hyperparameter,  $c$ ,  $s$  and  $cs$  are input content image, input style image and output stylized image,  $F(\cdot)$  is en-

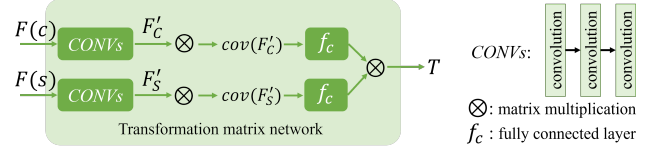


Figure 5: Feature transformation matrix network in [LLKY19].

coded feature map output from VGG encoder,  $F(\cdot) = F^{relu4\_1}(\cdot)$ ,  $F^l(\cdot)$  is intermediate feature output from layout  $l$  in VGG, and  $l_s = \{relu1\_1, relu2\_1, relu3\_1, relu4\_1\}$ . The style transfer network is trained with MS-COCO dataset [LMB\*14] as content images and painting pictures collected from WikiArt [PM11] as style images. Both datasets contain roughly 80,000 images. Though Huang and Belongie [HB17] found Gram matrix loss can produce similar results, they match IN statistics between style and stylized output.

To extend style transfer with more local awareness, SANet [PL19] and AdaConv [CZG\*21] propose local-aware mechanism for style fusion. AdaAttN [LLH\*21] propose a transformer to consider style feature transfer of both local and global awareness. Chen *et al.* [CWZ\*21] and Zhang *et al.* [ZTD\*22] utilize contrastive learning to improve local domain enhancement.

**Style Feature Transformation.** Another stream of arbitrary style transfer is to learn **feature transformation** between content features and output features [LFY\*17, LLL\*18, LLKY19]. Li *et al.* [LLKY19] proposed real-time **Linear Style Transfer (LST)** method, which investigates feature transformation learned from network for feature fusion rather than summary statistic matching (e.g., AdaIN). The work used a similar arbitrary style transfer framework as shown in Figure 4. Instead of using AdaIN to fuse content and style features, Li *et al.* [LLKY19] proposed to train an additional transformation network (Figure 5) with convolutions to learn an affine transformation matrix  $T$  from content features  $F(c)$  and style features  $F(s)$ . The transformed stylized features  $t$  is obtained by:

$$t = T \cdot (F(c) - \mu(F(c))) + \mu(F(s)), \quad (8)$$

and fed into the decoder to produce stylized image. Particularly, content feature  $F(c)$  is compressed and uncompressed through learnable convolution layers before and after the multiplication by the transformation matrix  $T$ . The whole network design and training content and style objectives can be similar to [HB17]. The network comprises a pre-trained and fixed VGG encoder, a trainable decoder, and additional convolution blocks for transformation matrix learning as well as for feature compression and uncompression. It is supervised by content and style losses computed from VGG (Eq. 2 and 3, or Eq. 7). The symmetric decoder is first trained to reconstruct the input images on MS-COCO dataset [LMB\*14]. Then the image reconstruction encoder-decoder module is fixed and the transformation module is trained with style images from WikiArt [PM11].

### 2.2.3. Image-to-Image Translation

Image-to-image translation (I2I) is a task to translate an image from one source domain to a target domain, which makes it applicable to visual style transfer. It usually requires partial preservation of



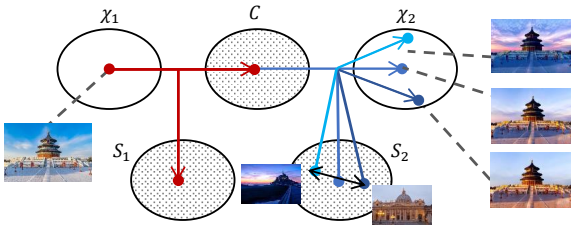


Figure 6: Disentanglement of content and style representations. It shows image-to-image translation from domain  $X_1$  to domain  $X_2$  with invariant content latent space  $C$  and variant style latent spaces  $S_1$  and  $S_2$ . An image in  $X_1$  is translated to different images in domain  $X_2$  by reassembling content code of input image and random style codes in target style latent space  $S_2$ . Images adapted from [CVS\*22].

the source content and generates target characteristics to match the translated image to the target domain.

**GAN-based Image-to-image Translation.** GAN [GPAM\*14] variants for image-to-image translation [IZZE17, ZPIE17, LBK17] focus more on domain-to-domain translation, and usually the model is not generic but task-specific. For example, if the model is trained with cat and dog images, the model is able to transfer cat to dog or dog to cat, and never able to transfer a human face to a dog or cat face. Different from pix2pix [IZZE17], CycleGAN [ZPIE17], UNIT [LBK17], etc. which model I2I problem as a deterministic one-to-one mapping without reference, multi-modal image-to-image translation models such as MUNIT [HLBK18], DIRT [LTH\*18] and DSMAP [CWC20] can theoretically synthesize unconstrained translated images with examples or given latent features. Multi-modal translation methods can work for the exemplar-based arbitrary style transfer problem.

Different from conventional arbitrary style transfer methods using pre-trained network for feature extraction (e.g., AdaIN, LST), multi-modal I2I translation methods train two feature encoders (e.g.,  $E_c, E_s$ ) for content and style domain from scratch. In general, content and style losses are the mean squared errors of embedded features between input content and output, input style and output. With the assumption of *disentanglement of content representation and style representation* in latent domains (see Figure 6), multi-modal image-to-image translation approaches [LTH\*18, HLBK18, LHM\*19, CWC20, CVS\*22] perform effective image translation with content appearance but target style.

Compared to traditional neural style transfer methods [GEB16, JAFF16, HB17], image-to-image translation models generate more high-fidelity images with more complex networks such as GANs, but the whole model is much more resource-consuming.

**Diffusion-based Image-to-image Translation.** Diffusion models [DN21, HJA20, SME21] is a type of generative models that progressively construct image content from Gaussian noise. As shown in Figure 7, diffusion models learn a consecutive denoising process and remove the noise step by step during image sampling. The randomness of the noisy training images provides extra data richness that facilitates the strong generation ability. We refer readers to the survey by Yang et al. [YZS\*23] for the basics in diffusion

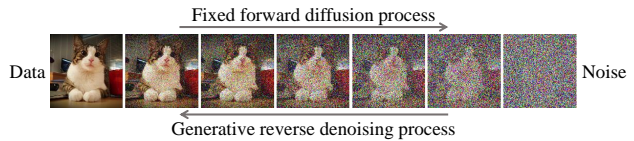


Figure 7: The forward and reverse process of diffusion models. In forward diffusion process, stronger random Gaussian noise is added to the image step by step. A neural network learns to denoise and thus recovers the image between any of these individual steps. Image adapted from [HJA20].

models and the recent survey by Po et al. [PYG\*23] for discussions of diffusion models in visual computing applications.

Diffusion models naturally support naive I2I translation. By adding certain levels of noise and then denoising the images, new image content is introduced, and the original image content is partially kept. However, part of the original image content is destroyed before any technical understanding mechanism in this naive approach, and thus some information from the source domain is no longer available. To address this issue, early methods [SCC\*22, BSSE21, SWB21] concatenate the source image with the noise map as input, and then follow the regular diffusion model training process. Su *et al.* [SSME23] manipulate the diffusion process to adapt the I2I translation setting. This method aims to train a source diffusion model and a target diffusion model on the source and target image domains, respectively. At testing time, a source image is first encoded by the source model to become a noisy version, and this noisy source image is then denoised by the target model to complete the I2I transfer. Li *et al.* [LXLL23] further integrate this separate image noising-and-denoising process into a sole diffusion model by sampling interpolations of source and target as ground truth for the middle generative steps.

The recent adoption of language models [RKH\*21] and the availability of text-image datasets [SVB\*21, SBV\*22] have led to the popularity of text-guided image diffusion models [RDN\*22, RBL\*22, SCS\*22]. These models concatenate the CLIP embedding of the text prompt to the image sample in diffusion model training, after which at inference allows plausible image generation conditioned on the text prompt. Follow-up methods [MHS\*22, PKSZ\*23] naively leverage the language setting of the pre-trained text-guided diffusion models for I2I translation. They add noise to the source image and then denoise it with a text prompt that describes the target features. Several I2I methods control the text prompts to transfer images [HMT\*22, KZL\*23]. They optimize in latent space a target text prompt that minimizes the distance to the source image. This optimized text prompt then activates the pre-trained diffusion models for content generation while preserving the original image features.

ControlNet [ZRA23] proposes possibly the most popular network architecture among diffusion-based I2I translation advances. It locks a pre-trained diffusion model and trains a dual learnable copy of this pre-trained model. The trainable copy receives the source image and from the locked model the target text prompt information. After feeding forward, the processed information is then injected back to the locked model to utilize the unchanged prior knowledge

and avoid overfitting. This method is adaptable for a wide range of customized source image types for I2I translation (e.g., hand sketch, stroke) and is efficient as all its modules starting from the pre-trained diffusion model require less re-training effort. Instruct-Pix2Pix [BHE23] solves the diffusion-based I2I translation problem from a more basic perspective by directly constructing a diverse image-prompt-image dataset. It uses LLM (e.g., GPT-3 [BMR\*20]) to generate text prompt pairs and uses [HMT\*22] discussed in last paragraph to generate image pairs. These pairs are then trained from scratch as in the usual diffusion process except for concatenating the source image to its first network layer.

### 2.3. Connection to Non-photorealistic Rendering

Since the middle of nineties, academics in computer science have aroused interest in visually appealing artworks, and they have been exploring studies on automatic artwork synthesis. In the community of computer graphics at that time, the development of NON-PHOTO-REALISTIC RENDERING (NPR) [GG01] inspired abstract stylized rendering for either 3D models, 3D images or 2D images, such as toon shading, Gooch shading [GGSC98], stroke-based painterly rendering [Hae90, Her98], patch-based texture synthesis and transfer [EF01, HJO\*01]. In the field of computer vision, early researchers introduced abundant NPR stylization (also known as artistic stylization) algorithms for images, transferring painterly style to photographs. Without neural networks, NPR stylization was achieved by post-processed rendering (e.g., toon and Gooch shading), procedural stroke-based and patch-based stylization [Aar18, KCWI12], etc. Traditional NPR techniques have been widely used in the realms of animation making and data visualization. However, these techniques only support low-level control of simple strokes and textures, and require handcrafted style patterns and rules. With the increasing development of neural networks, researchers have been probing more intelligent and automatic algorithms for digital stylization with the self-learning ability in machine learning, as known as neural style transfer (NST), which is the main focus of this report. NST techniques have achieved general stylization for seen or unseen arbitrary style targets, with high-level controllability with reference and semantics. Furthermore, NST offers higher speed for stylization production, which accelerates cinematic digital production [JSS17, NR21, HHK\*23] and accomplishes real-time stylization for VR [THC\*22] and AR [Tan19] applications (see Figure 2).

### 2.4. Background on 3D Neural Rendering

Equipped with background from 2D visual style transfer, let us now explore the background for 3D neural stylization. In this section, let us first briefly introduce neural 3D representations and then discuss neural rendering techniques.

#### 2.4.1. 3D Representations

Conventional 3D representations are mostly explicit representations, which includes triangle and polygon meshes, point clouds, occupancy grids, etc. It also contains some implicit representations such as signed distance functions and their truncated versions. With the advances of deep learning, there is a growing interest in using a

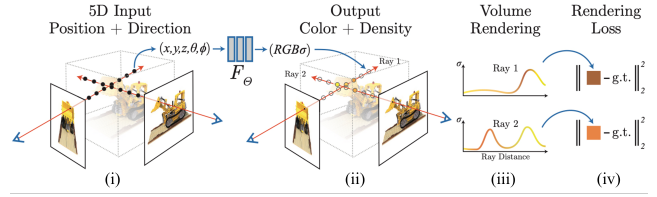


Figure 8: Neural radiance fields. A NeRF stores a volumetric scene representation as the weights of an MLP  $F_{\Theta}$  trained on multi-view images with known camera poses. Novel views are rendered by integrating the density and color at intervals along each viewing ray. Image adapted from [MST\*20].

neural network to represent 3D data as neural implicit representations. Traditional explicit representations are also widely employed to implicit 3D reconstruction in a hybrid manner to speed up 3D feature training and photorealistic rendering. Examples includes the hybrid representation of point clouds [RK21, KKLD23], voxel grids [MESK22, SSC22, FTC\*22], and mesh [CFHT23].

An important application of 3D representations is for view synthesis, which connects the 3D space to image representations. Recent advances in neural rendering have shown compelling potential for implicitly reconstructing 3D scenes from multi-view images via 3D-aware novel view synthesis techniques. Deep neural networks can learn 3D geometry and appearance features [RK20] and even directly represent a whole 3D scene [MST\*20]. For example, Riegler and Koltun [RK20, RK21] train a deep generative convolutional model mapping 3D point features from source views to target views with source multi-view features, freely producing photorealistic novel view images in the scene, Mildenhall *et al.* [MST\*20] adopted neural volumetric representation and proposed the revolutionary neural radiance fields with implicit continuous function to represent a 3D scene, which will be introduced in next section.

#### 2.4.2. Neural Radiance Fields

Neural radiance fields (NeRFs) [MST\*20] is a groundbreaking technique that models a complex 3D scene by learning from multiple views of the scene via differentiable volumetric rendering of the scene. Unlike traditional methods that rely on explicit 3D representations, NeRF employs neural networks to approximate the volumetric scene function, capturing both view-dependent appearance and view-independent geometry information. With its underlying scene representations and high-quality rendering, NeRF has opened up new possibilities for photorealistic rendering and its applications that require realistic and immersive 3D scene synthesis.

A typical NeRF scene is represented by a continuous function (MLP  $F_{\Theta}$ ) with 5D query input  $(x, y, z, \theta, \phi)$  comprised of spatial locating  $(x, y, z)$  and viewing direction  $(\theta, \phi)$ , and outputs estimated RGB radiance color  $c$  and density  $\sigma$ . A rendering of the scene can be performed with volume rendering techniques that query the network for density and color values at each sampling points  $t_i$  (at discrete uniform sampling intervals) along each viewing ray  $\mathbf{r}$  originated from the camera center to each image pixel. The final rendered color  $C$  along this ray is the integration of evenly-spaced  $N$  interval

radiances  $c_i$ :

$$C \approx \sum_1^N T_i \alpha_i c_i, \quad (9)$$

$$T_i = \prod_{j=1}^{i-1} (1 - \alpha_j), \alpha_i = 1 - e^{-\sigma_i \delta_j},$$

where  $T_i$  indicates how much radiance occluded earlier interval  $i$  along ray,  $\alpha_i$  indicates how much invisibility contributed by ray interval  $i$ ,  $\delta_j = t_{j+1} - t_j$  is the distance between adjacent samples. The fully-connected network  $F_\Theta$  can be trained with a mean squared error loss between the rendered and ground truth pixel colors.

Figure 8 illustrates the overview of NeRF representation, training and rendering process. From the observation of the low-quality rendering results, Mildenhall *et al.* [MST\*20] demonstrate two refinements to represent high-fidelity complex scenes, i.e., positional encoding for input coordinates [TSM\*20] and hierarchical sampling along the viewing ray, which encode high-frequency information of the scene. Fully connected networks are biased to learn low frequencies faster and the issue is alleviated by applying a simple mapping from low frequency to high frequent embedding for the network input [TSM\*20]. For the hierarchical ray sampling, authors jointly train two identical MLP networks for "coarse" and "fine" rendering with same rendering mean squared error loss, while coarse network provides weights as probability distribution for new finer samples in fine network. To get weights of coarse network, Eq. 9 is rewritten for the coarse network  $C_c(\mathbf{r})$  as a weighted sum of all sampled colors  $c_i$  along the ray  $\mathbf{r}$ :

$$C_c(\mathbf{r}) = \sum_{i=1}^{N_c} w_i c_i, \quad (10)$$

$$w_i = T_i (1 - e^{-\sigma_i \delta_i}).$$

These weights are normalized as  $\hat{w}_i = \frac{w_i}{\sum_{j=1}^{N_c} w_j}$  to obtain a piecewise-constant probability density function (PDF) along the ray. Then using inverse transform sampling,  $N_f$  important samples are taken from this distribution and optimize the "fine" network with all  $N = N_c + N_f$  samples. When rendering, final "fine" color of the ray  $C_f(\mathbf{r})$  is rendered using Eq. 9 from all  $N$  samples. During training, a photometric loss between rendered and ground-truth pixel values is computed by mean squared error.

**NeRF Extensions.** Naive NeRF is typically suitable for bounded scenes such as objects and small forward-facing scenes. To extend it to large unbounded scenes, Zhang *et al.* proposed NeRF++ [ZRSK20] to handle foreground and background separately with two NeRF networks. Due to the memory-intensive and low-efficient sampling in NeRF, explicit 3D representations [MESK22, FTC\*22, SSC22, CFHT23, KKLD23, CXG\*22] are exploited for quicker radiance field training and rendering, in the form of explicit field or hybrid field (explicit plus neural network). These discrete data representations benefit computation reduction, efficient use of network capacity, rendering speedup by empty skipping, and element manipulation [XTS\*22]. For example, voxel grid is used in Plenoxels [FTC\*22], InstantNGP [MESK22], DVGO [SSC22], TensorRF [CXG\*22], point cloud is used in 3D Gaussian Splatting [KKLD23], mesh is used in MobileNeRF [CFHT23]. But voxel grids constrain scene scale and cannot well perform for large unbounded scenes,

point cloud and mesh based representations are limited to memory resources. The fidelity of NeRF rendering can be further improved with anti-aliasing [BMV\*22a, BMV\*22b, BMV\*23], as well as lifting the assumption of piecewise-constant PDF in volume rendering to piecewise linear [UNY\*23].

### 3. 3D Neural Stylization

**Definition.** 3D neural stylization refers to the application of neural stylization techniques to modify the visual appearance and aesthetic characteristics of pre-existing 3D digital representations. This process involves leveraging neural networks and associated stylization algorithms to manipulate the visual and geometric attributes such as color, texture, and shape of the 3D models. 3D neural stylization facilitates the automatic generation of visually stylized renditions of 3D digital content, offering new avenues for creative expression and visual design in the field of computer graphics.

To fuse 3D representation with a new style, it is necessary to consider two important factors: 3D geometry preservation and style transformation. Similar to visual style transfer, we focus on image-based and text-based 3D neural stylization methods. Most methods rely on existing large pre-trained models (e.g., VGG and CLIP) for zero-shot feature extraction, and do not require any extra 3D data pre-training. Compared to pre-trained 3D feature extractors on 3D data (e.g., voxels [WSK\*15], meshes [MBBV15], point clouds [QSMG17, ZJJ\*21]), imagery and textual pre-trained models are widely accessible, and they are well-known for multi-level visual patterns and semantic feature extraction.

In this section, we first introduce a taxonomy for neural stylization and give an example of the categorization of existing 3D neural stylization methods. In the subsequent sections, we will introduce state-of-the-art 3D neural stylization techniques on diverse 3D representations, such as mesh, volumetric data, point clouds, and implicit fields, focusing on transforming appearance and/or geometry stylization. Finally, we summarize and analyze techniques in depth for 3D neural stylization.

#### 3.1. Taxonomy

We extend terminologies for 3D neural stylization from their 2D counterparts. A taxonomy for 3D neural stylization methods is shown in Figure 9 with details as follows.

- *Representations* could be explicit images or implicit 2D fields, built 3D assets such as mesh, volumetric simulation, 3D reconstruction from multi-views such as reconstructed mesh, and implicit 3D fields.
- *Neural Style Feature* indicates image visual embedding or textual semantic embedding from pre-trained feature extractors, typically neural classifiers.
- *Optimization* refers to optimization-based (similar to Section 2.1) or prediction-based stylization methods (similar to Section 2.2) with single, multiple, or arbitrary styles support.
- *Stylization Genres* refers to different types of stylization, from styles being retrieved from artwork such as paintings with abstract and artistic look and feel (e.g., the statue scene with van Gogh's starry night in Figure 1), or realistic styles including traditional color-based style transfer and photorealistic geometric



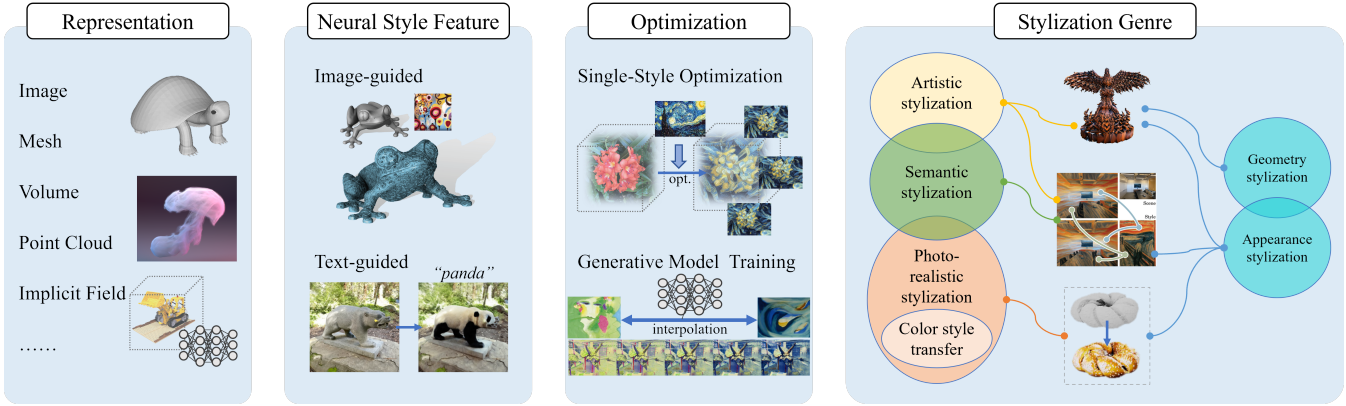


Figure 9: Taxonomy of 3D neural stylization. Images from [RMA\*23,AONA22,MST\*20,LTJ18,HTE\*23,ZKB\*22,LZC\*23,CSL\*23,PHY23].

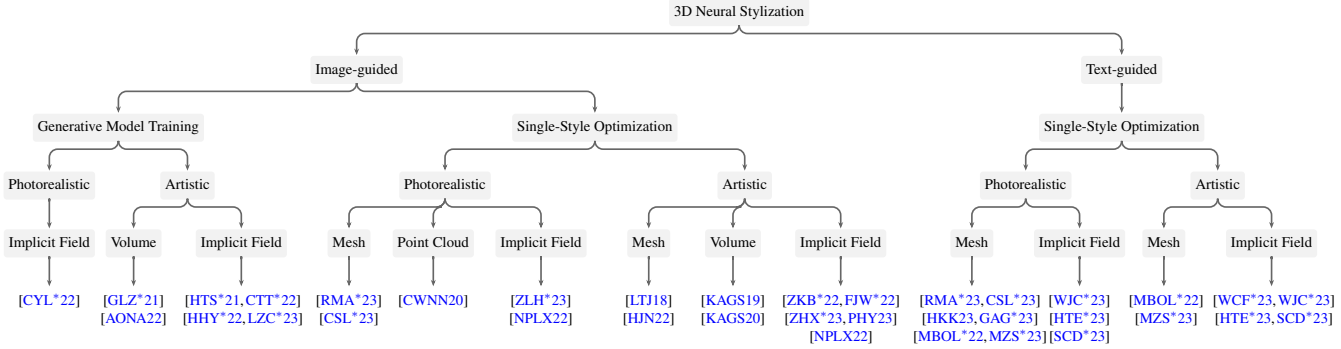


Figure 10: Hierarchical classification of 3D neural stylization methods.

and appearance changes (e.g., "burning pinecone" in Figure 1), to semantic style transfer with style semantic correspondence with explicit labels or masks, or implicit textual or visual semantic localization and mapping. We further classify methods into geometric stylization and appearance stylization, where geometry stylization indicates transforming the original shape to align style reference, such as altering positions of vertices, voxels, and appearance stylization refers to re-colorization, pattern and motif transfer upon such as image pixels, texture maps, vertex colors, point colors, and radiance fields.

Figure 10 shows a hierarchical classification of 3D neural stylization methods. Table 1 highlights in detail selected 3D stylization methods with categorization and comparison based on our proposed taxonomy criteria in Figure 9.

### 3.2. Neural Stylization on Mesh

Neural stylization on mesh with an image or (and) a textual style reference speeds up novel artwork design and style renovation based on a given mesh-based geometry. It takes as input a mesh with visual or textual style reference, and outputs the stylized textured mesh. Typical applications involve mesh geometry stylization [LTJ18], artistic or realistic texture stylization [HJN22,HKK23,RMA\*23,CSL\*23], and joint stylization of mesh

geometry and texture [KUH18,MBOL\*22,MZS\*23]. The resulting stylized meshes can be quickly rendered through conventional computer graphics pipeline, which allows various types of real-time applications such as VR.

#### 3.2.1. Geometric Stylization on Mesh Surface

3D neural stylization enables altering mesh geometry towards artistic visual patterns or into a target shape aligned with a visual reference or textual description. Such geometry edits assist creative 3D modeling such as engraving effect on surface [LTJ18] and geometry morphing [GAG\*23]. Existing works tend to learn geometry alternation in the form of vertex position displacement, some others learn displacement explicitly via differentiable rendering [LTJ18], while some learn transformation implicitly via neural networks [MBOL\*22,MZS\*23,GAG\*23].

Liu *et al.* [LTJ18] proposed *Paparazzi*, a differentiable rendering process that allows the propagation of changes in the image domain to changes in the mesh vertex positions. *Paparazzi* takes a triangle mesh as input, and applies image energy such as latent content and style losses [GEB16] between render image(s) and gray-scale style image to update vertex positions. After convergence, the mesh is stylized with artistic strokes and motifs in the style image.

Recently, researchers explored text-guided mesh stylization with CLIP loss (Eq. 4) controlling geometric and/or appearance

Method	Representation & Style Feature				Optimization		Runtime		Style Genre			Code			
	Input & 3D Repr	Ref	Output	Scene	G <sup>a</sup>	SS	DD <sup>b</sup>	FT <sup>c</sup>	RT <sup>d</sup>	NPS	PS	SM	TA	TG	</>
Liu <i>et al.</i> (Paparazzi) [LTJ18]	mesh	image	mesh	object	X	✓	X	X	✓	✓	X	X	X	✓	<a href="#">↗</a>
Höllein <i>et al.</i> (StyleMesh) [HJN22]	RGB-D views + reconstructed mesh	image	textured mesh	indoor room	X	✓	X	X	✓	✓	X	X	✓	X	<a href="#">↗</a>
Michel <i>et al.</i> (Text2Mesh) [MBOL*22]	mesh	text (or image)	vertex-colored mesh	object	X	✓	X	X	✓	✓	✓	✓	✓	✓	<a href="#">↗</a>
Ma <i>et al.</i> (X-Mesh) [MZS*23]	mesh	text	vertex-colored mesh	object	X	✓	X	✓	✓	✓	✓	✓	✓	✓	<a href="#">↗</a>
Hwang <i>et al.</i> (Text2Scene) [HKK23]	meshes + seg labels	image & text	vertex-colored mesh	indoor room w/ objects	X	✓	X	X	✓	X	✓	✓	✓	X	<a href="#">↗</a>
Gao <i>et al.</i> (TextDeformer) [GAG*23]	mesh	text	mesh	object	X	✓	X	X	✓	X	✓	X	X	✓	<a href="#">↗</a>
Richardson <i>et al.</i> (TEXTure) [RMA*23]	mesh	text or images	textured mesh	object	X	✓	X	✓	✓	X	✓	X	✓	X	<a href="#">↗</a>
Chen <i>et al.</i> (Text2Tex) [CSL*23]	mesh	text	textured mesh	object	X	✓	X	X	✓	X	✓	X	✓	X	<a href="#">↗</a>
Kim <i>et al.</i> (TNST) [KAGS19]	volume	image	volume	dynamic smoke	X	✓	X	X	X	✓	X	X	X	✓	<a href="#">↗</a>
Kim <i>et al.</i> (LNST) [KAGS20]	volume	image	volume	fluid	X	✓	X	X	X	✓	X	X	✓	✓	<a href="#">↗</a>
Guo <i>et al.</i> (SKPN) [GLZ*21]	volume	image	volume	dynamic or static model	✓	X	✓	X	✓	✓	X	X	✓	X	X
Aurand <i>et al.</i> (ENST) [AONA22]	volume	image	volume	smoke	✓	✓	X	X	✓	✓	X	X	X	✓	X
Cao <i>et al.</i> (PSNet) [CWNN20]	colored point clouds	image	colored point clouds	object	X	✓	X	X	✓	X	✓	X	✓	X	<a href="#">↗</a>
Huang <i>et al.</i> (LSNV) [HTS*21]	multi-views + depth maps (point)	image	novel views	bounded/unbounded scene	✓	X	✓	X	✓	✓	X	X	✓	X	<a href="#">↗</a>
Chiang <i>et al.</i> (HyperStyle) [CTT*22]	multi-views(NeRF)	image	novel views	unbounded scene	✓	X	✓	X	X	✓	X	X	✓	X	<a href="#">↗</a>
Huang <i>et al.</i> (StylizedNeRF) [HHY*22]	multi-views(NeRF)	image	novel views	bounded/unbounded scene	✓	X	✓	X	X	✓	X	X	✓	X	<a href="#">↗</a>
Liu <i>et al.</i> (StyleRF) [LZC*23]	multi-views(NeRF)	image	novel views	bounded scene	✓	X	✓	X	✓	✓	X	✓	✓	X	<a href="#">↗</a>
Chen <i>et al.</i> (UPST-NeRF) [CYL*22]	multi-views(NeRF)	image	novel views	bounded scene	✓	X	✓	X	✓	X	✓	X	✓	X	<a href="#">↗</a>
Zhang <i>et al.</i> (ARF) [ZKB*22]	multi-views(NeRF)	image	novel views	bounded/unbounded scene	X	✓	X	✓	✓	✓	X	X	✓	X	<a href="#">↗</a>
Fan <i>et al.</i> (INS) [FJW*22]	multi-views (NeRF, SDF)	image	novel views	bounded scene	X	✓	X	X	X	✓	X	X	✓	X	<a href="#">↗</a>
Nguyen-Phuoc <i>et al.</i> (SNeRF) [NPLX22]	multi-views(NeRF)	image	novel views	bounded/unbounded scene	X	✓	X	X	✓	✓	X	✓	✓	X	X
Zhang <i>et al.</i> (LipRF) [ZLH*23]	multi-views(NeRF)	image	novel views	bounded/unbounded scene	X	✓	X	✓	✓	X	✓	X	✓	X	X
Zhang <i>et al.</i> (Ref-NPR) [ZHX*23]	multi-views(NeRF)	edited view(s)	novel views	bounded/unbounded scene	X	✓	X	✓	✓	✓	X	✓	✓	X	<a href="#">↗</a>
Pang <i>et al.</i> (LocalStyleNeRF) [PHY23]	multi-views +seg maps(NeRF)	image	novel views	indoor room	X	✓	X	✓	✓	✓	X	✓	✓	X	<a href="#">↗</a>
Wang <i>et al.</i> (NeRF-Art) [WJC*23]	multi-views(NeRF)	text	novel views	bounded scene	X	✓	X	X	X	✓	✓	X	✓	✓	<a href="#">↗</a>
Wang <i>et al.</i> (TSNeRF) [WCF*23]	multi-views(NeRF)	text	novel views	unbounded scene	X	✓	✓	X	X	✓	X	✓	✓	X	X
Haque <i>et al.</i> (Instruct-N2N) [HTE*23]	multi-views(NeRF)	text	novel views	bounded/unbounded scene	X	✓	X	X	✓	✓	✓	✓	✓	✓	<a href="#">↗</a>
Song <i>et al.</i> (Blending-NeRF) [SCD*23]	multi-views(NeRF)	text	novel views	object	X	✓	X	X	X	✓	✓	✓	✓	✓	X

<sup>a</sup> Generative model indicates style transfer via feedforward neural networks. The opposite method is per-style-per-scene optimization.

<sup>b</sup> Large-scale reference style images or prompts are required for training.

<sup>c</sup> Training time can reach less than 10 minutes to get plausible results on a common non-commercial GPU.

<sup>d</sup> Inference speed with less than 1 second per image transfer in the resolution of  $256 \times 256$ .

Table 1: A detailed summary of 3D neural stylization methods. **G** stands for **Generative** model training, **SS** stands for **Single** (or **Several**) **Style(s)** per scene, **DD** stands for visual or textual **Data-Driven** training, **FT** stands for **Fast Training**, **RT** stands for **Real-Time** rendering at inference, **NPS** stands for **Non-Photorealistic** (or **Artistic**) **Style Transfer**, **PS** stands for **Photorealistic Style Transfer**, **SM** stands for **Semantic consistent Match**, **TA** stands for **Transfer** (or **Optimize**) **Appearance** feature, **TG** stands for **Transfer** (or **Optimize**) **Geometry** feature.

changes [MBOL\*22, MZS\*23]. *Text2Mesh* [MBOL\*22] and *X-Mesh* [MZS\*23] incorporate a new concept of Neural Style Field (NSF), which is composed of an MLP network that maps vertex coordinates to vertex color (offset) and vertex position offset. The stylized mesh with updated point colors and point positions is rendered into multiple colored and gray-scale images, which are used for computing CLIP loss against a given text prompt. Michel *et al.* [MBOL\*22] proposed a new training strategy for text-guided 3D stylization with NSF. The strategy includes the utilization of a neural style field network with positional encoding, training view transformation augmentation, and geometry-only loss enhancement. They found neural style field better stylizes mesh than straightforward explicit mesh optimization does. The follow-up work *X-Mesh* of Ma *et*

*al.* [MZS\*23] explores a similar but more efficient training scheme for text-guided mesh stylization. Ma *et al.* upgrade the neural style network with a Text-Guided Dynamic Attention Module (TDAM) using dynamic linear layers after positional encoding, which takes as input both the vertex coordinate encoded feature and text CLIP embedding, and calculates text-vertex attention at both channel and spatial levels. With the proposed attention module, *X-Mesh* achieves fast convergence in a few minutes for high-quality stylized results. *TextDeformer* by Gao *et al.* [GAG\*23] upgraded the local CLIP-guided mesh geometric stylization [WCH\*22, MBOL\*22, MZS\*23] through Jacobians [AGK\*22] for global and smooth mesh deformation. Instead of learning position displacement directly, they assign Jacobians by matrices for each triangle and solve a Poisson

problem [AGK\*22] to compute the according vertex deformation map, which largely achieves deformation with low-frequency to high-frequency details.

The discussed works [LTJ18, MBOL\*22, MZS\*23] require a camera sampling strategy for training when given a sole mesh for stylization. For example, in *Paparazzi* cameras are uniformly sampled on an offset surface positioned at a fixed distance from the shape. The cameras on the offset surface maintain a fixed distance from the given shape and face inward along vertex normals. This camera placement technique helps to minimize bias towards specific views, ensures smooth camera views around sharp edges, and achieves full coverage for the majority of the shapes. Michel *et al.* [MBOL\*22] devised a new training view selection scheme. They render the 3D mesh from various viewpoints distributed uniformly around a sphere and computed the CLIP similarity between each view and a target text prompt. The view with the highest CLIP similarity is designated as the anchor view. During training, multiple views (typically 5) are randomly sampled using a Gaussian distribution centered around the anchor view. The CLIP embeddings across all views are averaged as the CLIP loss for training, thereby encouraging view consistency. Furthermore, the sampled views are augmented with a random perspective (or) and a random crop operations, which avoids suboptimal stylization.

### 3.2.2. Appearance Stylization on Mesh Texture

Mesh texture represents the complex visual appearance with color and patterns, for which neural style transfer techniques (Section 2) are well developed. By supervising texture transformation and synthesis via visual feature extractors or generative models, there appear some promising works for mesh texture stylization [HJN22, LZJ\*22, RMA\*23, CSL\*23].

With an image in target artistic style, Höllein *et al.* [HJN22] proposed a depth- and angle-aware texture optimization scheme for 3D reconstructed mesh, called *StyleMesh*, which realizes plausible artistic pattern and stroke transfer on 3D semantic surfaces. *StyleMesh* optimizes an explicit texture image by backpropagating gradients computed from 2D content and style losses for each view of the scene (Eq.2 and Eq.3 of [GEB16]). Different from prior works such as [KUH18, MPSO18] that used differentiable rendering to transfer image style to texture via direct multi-view mapping and optimization, *StyleMesh* incorporates 3D-aware stylization by leveraging depth and surface normal information derived from the mesh. It largely mitigates artifacts such as view-dependent stretch and size artifacts that commonly arise from conventional 2D losses in 3D scenarios (see surface stretching example in Figure 11). *StyleMesh* realizes room-scale mesh artistic stylization with 3D awareness. However, it largely relies on posed images and ground-truth depths, and only stylizes reconstructed scenes.

Style descriptions with CLIP supervision enable optimizing mesh appearance colors such as [MBOL\*22, MZS\*23] (Section 3.2.1). Instead, *TANGO* [LZJ\*22] tends to optimize material parameters by CLIP supervision. It trains MLPs given the point and its normal to generate SVBRDF parameters and normal offset, which enables photorealistic rendering and 3D appearance style transfer with material optimization. However, solely harnessing the power of CLIP for stylization may not achieve realistic results

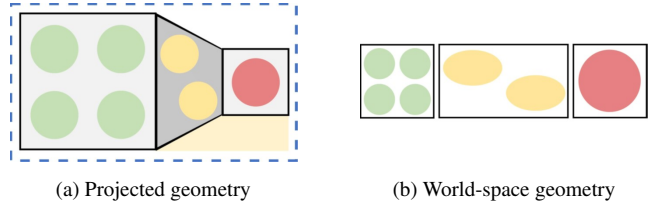


Figure 11: Stretched pattern artifacts from stylization in screen space. Image adapted from [KUH18].

[MBOL\*22, LZJ\*22, MZS\*23]. The increasing popular text-to-image diffusion models enable photorealistic and high-fidelity imagery synthesis, and recent works have started to explore diffusion for 3D element synthesis [PBJM23, WDL\*23, WLW\*23, LGT\*23, XWC\*23, CCJJ23, MRP\*23] or stylization [RMA\*23, CSL\*23].

Richardson *et al.* [RMA\*23] proposed *TEXTure*, a text-guided 3D texture painting scheme that iteratively draw the texture in view-by-view manner. To maintain 3D consistency, each view drawing iteration is guided by a view-dependent trimap mask that indicates the "keep", "refine", and "generate" regions of the texture map. Such trimap in a new view iteration is treated as a confidence map to control the amount of newly generated content for the current texture. Alongside the trimap, a rendered RGB and depth map are fed into a pre-trained depth-to-image diffusion model [ZRA23] to obtain a synthesized view. This synthesis is finally projected back to the texture map via optimization. Apart from texturing, the scheme of *TEXTure* is applicable for various tasks such as texture transfer, texture editing, and multi-view image transfer. Another concurrent work *Text2Tex* [CSL\*23] inpaints likewise the texture images from different views progressively with the help of the confident trimap and a depth-to-image diffusion model [ZRA23]. Compared to *TEXTure*, *Text2Tex* presets some axis-aligned viewpoints and alternatively updates the next best view which provides a more robust automatic view scheduling strategy that better addresses the blurriness and stretching artifacts.

One current issue is that these text-guided 3D stylization methods [MBOL\*22, MZS\*23, LZJ\*22, RMA\*23, CSL\*23, GAG\*23] are applicable on low-quality arbitrary meshes. Settings under larger-scale mesh with geometric and/or appearance stylization are still under-explored. Hwang *et al.* [HKK23] proposed *Text2Scene* to explore part-aware stylization on individual object meshes in an indoor scene with both image and text conditions. *Text2Scene* initializes scene color in line with the color histogram of the given reference image, and stylizes objects further with detailed texture in line with appearance style textual description. In particular, it separates an indoor scene with structure components (e.g., walls, ceilings, floors) and objects for part-aware stylization. *Text2Scene* constrains the whole scene in a similar style with a fixed appearance text prompt for individual objects, but it may lead to the disharmonious context of the whole space.

### 3.3. Neural Stylization on Volumetric Simulation

Kim *et al.* explored image-guided neural style transfer on volumetric simulation, particularly dynamic smoke [KAGS19] and flu-



ids [KAGS20]. In [KAGS19], they use pre-trained Inception CNN model [SVI\*16] as the single-view feature extractor, and apply content loss (Eq. 2) for semantic style transfer and style loss (Eq. 3) for abstract style transfer. They proposed a transport-based neural style transfer (TNST) method on grid-based voxels to optimize a velocity field (i.e., voxel movement) from several multi-views from Poisson sampling around a small area of the trajectory, and use a differentiable smoke renderer to render grayscale images to represent pixel-wise volume density. For temporal consistency among frames during smoke simulation, they compose a linear combination of the recursive aligned velocity fields of neighbor frames for the velocity field of the current frame. Later in [KAGS20], they adopt particle-based attributes from multi-scale grids, and optimize attributes of positions, densities and color per particle, which intrinsically ensures better temporal consistency than recursive alignment of velocity fields [KAGS19]. It largely improves efficiency by directly smoothing density gradients in stylization from adjacent frames for temporal consistency, and by stylizing only keyframes and interpolating particle attributes in-between.

Subsequently, Aurand *et al.* [AONA22] proposed to use a feed-forward network to avoid expensive iterative optimization in [KAGS19, KAGS20] and achieve fast volumetric stylization, reaching production level [KAOT23, HHK\*23]. Guo *et al.* [GLZ\*21] proposed an arbitrary appearance style transfer model for volumetric simulation via a volume autoencoder.

### 3.4. Neural Stylization on Point Clouds

*PSNet* [CWNN20] is a PointNet-based [QSMG17] stylization network specialized for point cloud color and/or geometry style transfer with a point cloud example (geometry and/or color transfer) or an image example (only color transfer). Similar to representing content and style features from a pre-trained model [GEB16], *PSNet* uses a PointNet-based classifier with two separate shared MLPs to extract intermediate outputs as geometry/content representation and regard the Gram-matrix of these outputs as appearance/style representation. The classifier is pre-trained on DensePoint dataset [LFM\*19]. *PSNet* utilizes point-cloud-based content and style losses (Eq. 2 and 3) to optimize geometry and/or appearance color of the source point cloud, simply replacing VGG features by *PSNet* features. In particular, content and style losses simultaneously apply to either geometry or appearance features. Since the Gram-based style representation is invariant to the number or the order of the input points, an example style image treated as a set of points can stylize source colored point cloud with only target color style without shape alternation.

### 3.5. Neural Stylization on Novel View Synthesis

Early works in stylization on novel views include stereoscopic image style transfer [CYL\*18, GHM\*18] and light field photo stylization [HMG20] with narrow-parallax viewpoints and holistic scene novel view stylization [HTS\*21]. Blending neural style transfer to novel view synthesis is an increasingly attractive topic [HTS\*21, MWL22, ZKB\*22] given the development of fast novel view synthesis techniques [WGSJ20, RK20, RK21, FTC\*22] and their applications [TLC22, THC\*22].

For example, Huang *et al.* [HTS\*21] explored 3D large scene

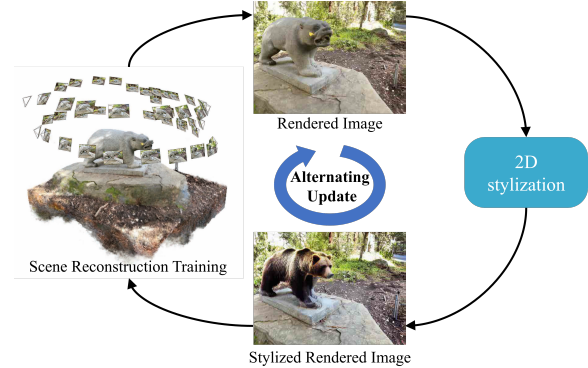


Figure 12: General framework for alternating updating 2D and 3D styles [NPLX22, HTE\*23]. Images adapted from [HTE\*23].

stylization as a novel view stylization problem. They found the simple combination of existing 2D stylization and novel view synthesis methods would lead to blurry, short-range and long-range inconsistent results. Instead, they proposed *LSNV*, a feed-forward point cloud feature transformation model for large-scale 3D scene stylization. They use a point cloud to represent scene features and aim to achieve point cloud feature linear transformation [LLKY19] from the source scene to the stylized scene. They adopt similar transformation network architecture (Figure 5) and feature transformation algorithm (Eq. 8) in LST [LLKY19], but feed point cloud features instead of image pixel-wise features for style transformation. As pre-processing, they reconstruct the scene, get point cloud and depth maps, and then project multi-view VGG *relu3\_1* features back to the reconstructed point cloud to obtain source scene 3D point cloud features. After transforming source point cloud features via the transformation network, they group and feed new features with a radius to MLPs and get aggregated stylized features for the final decoder’s rendering. They pre-train this novel view rendering decoder to reconstruct the non-stylized novel views for arbitrary scenes, and then they train the transformation network with the fixed decoder using content and style losses (Eq. 2 and 3) [GEB16, JAFF16] on WikiArt dataset [PM11]. Such a point cloud based novel view stylization supports relatively large-scale scenes based on [RK20], which supports arbitrary scene novel view synthesis after training.

### 3.6. Neural Stylization on NeRFs

In this section, we explore neural stylization on neural radiance fields (NeRFs), which has emerged as an important implicit scene representation that can be effectively learned from multi-view data.

#### 3.6.1. Optimization-based Stylization on NeRFs

Similar to visual style transfer, optimization-based stylization methods for NeRFs can support single or multiple target styles using visual or textual reference. Most single-style optimization approaches [ZKB\*22, FJW\*22, ZHX\*23, PHY23] proposed to reconstruct the scene including geometry and appearance from posed multi-views before stylization, and then fix or self-distill the geometry during optimization to stylize the appearance. Some NeRF-based meth-

ods [NPLX22, WJC\*23, HTE\*23] showed that it is also possible to update the geometry during stylization.

**A General Optimization Framework.** Nguyen-Phuoc *et al.* [NPLX22] proposed *SNeRF*, a *general alternating optimization pipeline* (Figure 12) for novel view stylization by arbitrary off-the-shelf 2D style transfer methods and any NeRF methods. They first reconstruct the scene using NeRF with original content multi-views, then iteratively stylize rendered multi-views and use stylized views to fine-tune the NeRF in a loop. After some iterations, the NeRF gradually becomes 3D-aware stylized. Extensive experiments validated the flexibility of this pipeline, which supports off-the-shelf 2D style transfer for any NeRF or NeRF variants. Theoretically, it supports either artistic or photorealistic style transfer. However, *SNeRF* requires optimization to be performed for numerous iterations, which takes a long time to complete. Later, Haque *et al.* [HTE\*23] explored the general framework for text-guided NeRF editing and introduced *Instruct-NeRF2NeRF* to edit an existing NeRF using 2D diffusion priors [BHE23]. Similar to *SNeRF* [NPLX22], they iteratively update a rendered view at a NeRF training viewpoint through an off-the-shelf image-to-image diffusion model, e.g., Instruct-Pix2Pix [BHE23]. The NeRF training then continues on the modified training dataset with the updated views. Such dataset updates and NeRF training happen frequently in turn. By assigning random strengths of noises to the updating views and as training goes, the NeRF gradually converges to a consistent 3D scene in the target style. Such a strategy of alternating style updates between 2D training data and the 3D scene (Figure 12) demonstrates generalizability to diverse scenes and enables fine-grained control over the stylization of NeRF using natural language.

**Image-based Optimization.** Zhang *et al.* [ZKB\*22] observed that feed-forward stylization approaches [HB17, LFY\*17] (Section 2.2.2) achieve zero-shot arbitrary style transfer after training, but these methods often struggle with faithful stylistic features like color and brushstrokes. Therefore, they turned to single-style optimization techniques for high-quality artistic stylized radiance fields, and introduced nearest neighbor feature matching (NNFM) style loss [KKP\*22] for 3D stylization. NNFM is a pixel-wise nearest-neighbor feature matching between style reference and rendered image via minimizing the cosine distance on VGG features, as shown in Figure 13. NNFM loss is defined as:

$$\mathcal{L}_{nmfm} = \frac{1}{N} \sum_{i,j} \min_{i',j'} \text{CosSim}(F(cs)_{ij}, F(s)_{i'j'}). \quad (11)$$

where  $F(\cdot)_{ij}$  denotes feature vector at pixel location  $(i, j)$  of  $F(\cdot)$ . Artistic radiance field (*ARF*) approach by Zhang *et al.* [ZKB\*22] optimizes and stylizes a reconstructed implicit scene (with frozen geometry branch) with an exemplar style image, under the supervision of content loss (Eq. 2) between rendered image and original training view and NNFM style loss (Eq. 11). To alleviate GPU memory cost and allow full-resolution computation loss, *ARF* proposed *deferred back-propagation* strategy to defer full-resolution gradient from the full-resolution rendering stage to the patch-wise re-rendering stage. *ARF* technique can apply to different implicit radiance field representations such as NeRF [MST\*20], Plenoxels [FTC\*22], TensoRF [CXG\*22]. The NNFM loss was validated more visually appealing in 3D stylization than typical Gram matrix loss [GEB16] or CNNMRF loss [LW16].

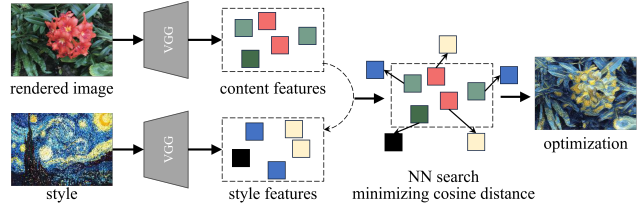


Figure 13: Nearest neighbor feature matching (NNFM) for artistic radiance field optimization. Image adapted from [ZKB\*22].

Even though *ARF* [ZKB\*22] realizes automatic nearest latent style feature matching with compelling stylistic details in 3D stylization, it lacks explicit semantic correspondences. Therefore, Zhang *et al.* proposed a reference-based non-photorealistic radiance field (*Ref-NPR*) [ZHX\*23]. Given a pre-trained radiance field, and a structure-preserved edited view, *Ref-NPR* builds a reference dictionary in a form of a cubic  $256^3$  voxels from the stylized reference view and corresponding estimated depth from radiance field. The dictionary maps any 3D point position to a discrete voxel with or without reference color. *Ref-NPR* registers all rays of training views to the closest intersection point dropping into the same voxel. For the occluded regions, they propose to search nearest-neighbor feature matching (NNFM in Figure 13) [KKP\*22, ZKB\*22] between other view and the reference view in training data, and replace features of rendered other views by features of edited reference view using identical indexing from previous feature matching. Further, to eliminate color mismatch, they transfer the average color in a patch at feature-level resolution by a coarse color matching loss following the previous NNFM. The final optimization of non-photorealistic radiance field (Plenoxels [FTC\*22] with frozen density but without viewing direction input) is supervised by explicit ray registered color, implicit matched feature, and patch-wise average color.

Referring to the disentanglement of content and style representations for style transfer (Figure 6), Fan *et al.* [FJW\*22] proposed to disentangle scene content and reference style features in neural fields with two separate networks. They use a model consisting of a style MLP module (SIM) and a content MLP module (CIM) to separately encode the representations of the style image and input scene, and an amalgamation MLP module (AM) to output both final color and density fusing style and content features. They first train a teacher NeRF model for reconstruction and then fix it during the stylization training stage for distilling density. In the stylization training stage, they optimize all modules by supervising color with content and style losses (Eq. 2 and 3), and supervising density from the teach model. [FJW\*22] has been verified as generalizable on different 2D (SIREN) or 3D (NeRF and SDF) scenes using the disentanglement scheme of content and style features on stylization. Different from [FJW\*22], Pang *et al.* [PHY23] disentangle content (geometry) and style (appearance) feature for only the given scene [CTT\*22, HHY\*22, CYL\*22] and introduced a dual NeRF model with geometry and appearance branches (similar to Figure 6 and 14), based on InstantNGP [MESK22]. Further, Pang *et al.* consider semantic style matching and add additional segmentation output in the geometry branch with an extra segmentation MLP after hash encoding. Training has two stages, the first stage is to recon-

struct NeRF and segmentation from posed RGB and segmentation multi-views for both branches, where segmentation is supervised by cross-entropy loss. In the second stage, they only fine-tune the appearance branch and optimize the NeRF appearance using NNFM loss (Eq. 11) [ZKB\*22] on mapped regions and content loss (Eq. 2). They particularly experimented on indoor scenes with pre-computed segmentation. Fan *et al.* [FJW\*22] and Pang *et al.* [PHY23] both proposed to use conditional style representations by feeding a one-hot vector or style index to the neural field, enabling conditional stylization for several styles.

Apart from the discussed artistic style transfer works above, Zhang *et al.* [ZLH\*23] analyzed the problem of 3D photorealistic stylization in terms of structure preservation and multi-view consistency, and found two criteria: nearby pixels in an image belong to same region if pixel values are close enough, and a point observed by two adjacent views should have close rendered color values from two views. They demonstrated that these demands can be fulfilled by solving a *Lipschitz-constrained linear mapping* problem over scene appearance representation. Therefore, they proposed *LipRF*, a learning framework that upgrades off-the-shelf 2D photorealistic style transfer (PST) methods with Lipschitz mapping tailored for 3D scenes. Similarly, they reconstruct a grid-based radiance field [FTC\*22] with separate geometry and appearance branches and fix the geometry branch during stylization training. *LipRF* uses a Lipschitz MLP to replace the linear mapping, and transform the radiance appearance field during the stylization training stage. In the stylization stage, stylized views by arbitrary 2D PST methods [YUC\*19, WZDB22] are used to supervise rendered stylized views to train the Lipschitz MLP. Since Lipschitz MLP needs to transform spherical harmonic coefficients on all vertices of voxel grids, which is GPU memory-hungry. To this end, they proposed the gradual gradient aggregation back-propagation strategy, which gradually aggregates gradients in a batch-wise way. Thus, the optimization process can be finished in a few minutes on average.

**Text-based Optimization.** The recent increasingly developed large-language models (LLM) and text-to-image diffusion models inspire the community to develop works on text-guided or text-to-image guided 3D scene stylization and editing [WCH\*22, WJC\*23, WCF\*23, SCD\*23, BZY\*23, HTE\*23, SFHAE23, ZWL\*23, SKH\*23]. Here we provide a brief discussion on the latest advances of text-guided NeRF stylization.

Wang *et al.* [WJC\*23] proposed *NeRF-Art* for *text-guided NeRF stylization with profound semantics*. Unlike simple color and shape stylization for objects in CLIP-NeRF [WCH\*22] using a CLIP-based matching loss (Eq. 4), *NeRF-Art* realizes complex stylization on diverse shapes and scenes, such as turning a human face into a Tolkien elf. Wang *et al.* proposed to fine-tune the pre-trained NeRF [YGKL21] using relatively direction CLIP loss [PWS\*21, GPM\*22] (Eq. 5), local and global contrastive CLIP-based loss, perceptual loss [JAFF16] and a weight regularization [BMV\*22a] for sharper details. While the directional CLIP loss can guide the style transformation, the stylization strength is still insufficient to alter a pre-trained NeRF model. To address this, they utilized the contrastive learning strategy to consider both positive (target text prompt) and negative samples (irrelevant text prompts) into account, and apply contrastive loss [CKNH20] in CLIP space. The whole

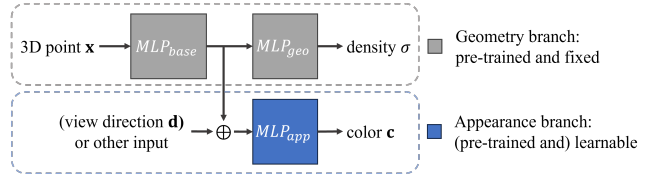


Figure 14: Canonical NeRF with geometry and appearance branches in 3D stylization [CTT\*22, HHY\*22].

rendered view and random cropped view patches [PEZZ20] are used for global and local contrastive losses, respectively.

Song *et al.* [SCD\*23] introduced *Blending-NeRF*, a text-guided NeRF-based blending model that enables localized style changes in specific spatial regions of an object. The style is formulated into three different types of variation, including appearance color changes, geometric density addition and density removal. To identify the regions for stylization, they leverage CLIPSeg [LE22], a pre-trained vision-language model, and employ a region loss for supervision. The stylization process involves two NeRF networks: the editable NeRF, responsible for stylizing the masked region with outputs for density, color, and extra density and color ratios, and the pre-trained source scene NeRF, which remains fixed during optimization. They particularly supervise the opacity degrees (summed weights in Eq. 10) of color changes, density addition, and density removal with a threshold. The end-to-end optimization is primarily guided by CLIP losses (Eq. 4 and 5), segmentation region loss, and additional opacity loss and regulation loss, with both rendered patch and text prompt augmentation. Notably, *Blending-NeRF* support different NeRF-based representations, including naive NeRF [MST\*20] and InstantNGP [MESK22].

While most text-guided NeRF stylization works focus on common semantic editing [WJC\*23, SCD\*23, HTE\*23], *TSNeRF* by Wang *et al.* [WCF\*23] particularly focuses on **abstract artistic** 3D stylization on NeRF with semantic textual descriptions of expected style. They introduced a semantic contrastive loss harnessed with CLIP, and fine-tuned CLIP with ArtBench artwork database [LLLK22] for accurate artistic textual embedding. Similarly, Wang *et al.* used the geometry branch and the appearance branch with a hypernetwork for NeRF stylization (Figure 14), with separate reconstruction and stylization stages. To alleviate the local minima by CLIP loss [GPM\*22] (Eq. 4) and over-stylization by directional CLIP loss [PWS\*21] (Eq. 5), they proposed a CLIP-based contrastive loss taking negative samples into account, similar to the strategy in *NeRF-Art* [WJC\*23]. Differently, they define positive and negative text samples and also consider CLIP-space direction from source image to target/source text as positive and negative directions. In the stylization stage, *TSNeRF* is supervised by photometric [MST\*20] and content loss [GEB16], cosine similarity loss between CLIP style embedding and that in ArtBench [LLLK22], and the proposed contrastive loss. Particularly, out of memory-intensive computation for full image, they render patches of the image, compute losses on stitched full image, and back-propagate gradients on patches.



### 3.6.2. Arbitrary Style Transfer on NeRFs

Using neural field as implicit scene representation such as NeRF, researchers started to explore arbitrary style transfer [CTT\*22, HHY\*22, LZC\*23] for a NeRF scene. It also involves the geometry reconstruction training phase (i.e., NeRF training) and then NeRF stylization training phase. Chiang *et al.* [CTT\*22] proposed to transfer arbitrary style to novel views on NeRF representation (NeRF++ [ZRSK20]). In the reconstruction phase, they utilize NeRF to disentangle geometry (density output) and appearance (view-dependent color output) into two output branches (as illustrated in Figure 14). In the stylization phase, they fix the geometry branch and regress the updated weights of the appearance branch via an MLP hypernetwork [HDL16] with the image style feature input extracted from a pre-trained style transfer VAE encoder. Since NeRF++ cannot support high-resolution image rendering at a fast speed, they propose to do patch sub-sampling [SLNG20] to compute content and style losses (Eq. 7) [HB17]. In that case, they can train stylized NeRF with small patch renderings. It accomplishes stylization on large outdoor 360° unbounded scenes, but limits the performance due to the low reconstruction quality of NeRF++ at that time. Since [CTT\*22], the two-stage training strategy became a standard and useful training pipeline for NeRF stylization.

*StylizedNeRF* by Huang *et al.* [HHY\*22] and *StyleRF* by Liu *et al.* [LZC\*23] are another two recent 3D arbitrary artistic style transfer works. *StylizedNeRF* applies a mutual learning strategy for 2D arbitrary style transfer model (e.g., AdaIN model [HB17]) and NeRF [MST\*20], encourages arbitrary style transfer model multi-view consistent and stylizing NeRF appearance. Specifically, they pre-train the style transfer model with 3D awareness under the supervision of multi-view content loss and style loss (Eq. 7), and additional proposed consistency loss with warping and estimated depth by reconstructed NeRF. The arbitrary style transfer model thus distills initial 3D consistent knowledge from NeRF. During the mutual learning stage, they fix ordinary NeRF’s geometry branch and use another MLP as a new appearance branch with the input of point position and learnable latent style codes. The style codes are optimized to be close to VGG style feature distribution extracted from a pre-trained style VAE encoder with a feature distribution loss. Finally, the pre-trained style transfer network and stylized NeRF are optimized together with the discrepancy penalty between output 3D inconsistent and consistent views.

*StyleRF* [LZC\*23] uses a similar style transformation scheme to *LSNV*, it learns a 3D feature grid lifted from pre-trained VGG, and then runs 3D stylization with a style transformation module [LLKY19] and a decoder for novel view synthesis. They obtain the feature map of each view via volume rendering (Eq. 9), and then apply linear style transformation [LLKY19, HTS\*21] on weighted features depending on the sum weight of sampled points along each ray (see  $w_i$  in Eq. 10). Finally, they adopt a 2D CNN decoder to generate stylized views. Similarly, *StyleRF* conducts two-stage training, the stage of feature grid learning and reconstruction without viewing direction input (based on TensorRF [CXG\*22]), and the stage of stylization training with fixed geometry. *StyleRF* also illustrated its advantage of data-driven style training for style interpolation and multi-style transfer with a 3D mask.

While arbitrary artistic style transfer for NeRF has been explored

	Literature	Scene	Cam	#View	Aug	Planning Criteria
Mesh	[LTJ18]	object	orth.	1	✗	uniform on offset surface, face vertex normal
	[MBOL*22]	object	pers.	5 <sup>a</sup>	✓	text-guided anchor view, sample around anchor
	[HKK23]	object	pers.	20 <sup>b</sup>	✓	random sample, evenly cover whole scene
	[RMA*23]	object	pers.	8 <sup>b</sup>	✗	around object (incl. top/bottom)
	[CSL*23]	object	pers.	6+20 <sup>b,c</sup>	✗	axis-align, face surface normal
Volume	[KAGS19]	object	orth.	9	✗	look at object, sample around a path
	[GLZ*21]	object	pers.	4	✗	random sample in a path
	[AONA22]	object	pers.	1	✓	sample in a path

<sup>a</sup> total views equals views per iteration;

<sup>b</sup> total views;

<sup>c</sup> 6 views for generation, 20 out of 36 predefined views for refinement.

Table 2: Summary of training view planning in selected 3D neural stylization methods. "Cam" refers to camera type such as orthogonal or perspective camera. "#View" is the sample number of views for each iteration/frame, unless indicated otherwise. "Aug" indicates rendered view augmentation.

in some previously discussed works [HTS\*21, CTT\*22, HHY\*22, LZC\*23], *UPST-NeRF* [CYL\*22] is the first arbitrary photorealistic style transfer work for 3D implicit scene, with similar separate geometry and appearance branches (Figure 14). For efficiency, Chen *et al.* [CYL\*22] proposed to use voxel grid representation based on DVGO [SSC22]. The scene contains two voxel grids, one is the density voxel grid for geometry, and the other is the feature voxel grid followed by a shallow MLP ( $MLP_{rgb}$ ) for predicting appearance color. Inspired by [CTT\*22], they used a hypernetwork to map VGG embedded style image features to weights of an additional hyper MLP of which the output is the input of  $MLP_{rgb}$ . *UPST-NeRF* conforms to two training stages, after reconstruction training, density and feature voxel grids are fixed, and only hypernetworks and  $MLP_{rgb}$  are learnable. During stylization training, stylized views by a fixed and pre-trained 2D photorealistic arbitrary style transfer network are used to supervise rendered views.

Compared to works based on common NeRF [CTT\*22, HHY\*22], *StyleRF* and *UPST-NeRF* are built on TensorRF and DVGO in voxel grid representation, which supports fast training and rendering and higher resolution of training patches, but may not work well for large unbounded scenes due to the grid-based representation.

### 3.7. Robustness

This section discusses practical aspects of 3D neural stylization methods, including view consistency, controllability, generalization, and efficiency.

#### 3.7.1. View Consistency

Different from 2D neural stylization, which concerns pixel-wise chrominance values and planar geometry such as 2D edges, 3D stylization requires 3D geometric consistency. Stylization on 3D

data for similar tasks such as appearance artistic or photorealistic stylization while preserving 3D consistency is challenging.

**View Planning.** Stylization on 3D data without camera planning or posed multi-view images, such as mesh [LTJ18, MBOL\*22, MZS\*23, HKK23, RMA\*23, CSL\*23, GAG\*23], volumetric simulation [KAGS19, KAGS20, GLZ\*21, AONA22], demands for planned viewpoints when supervised by multi-views. Table 2 summarizes some view planning strategies of mesh and volumetric stylization works. Since these works only focus on a single object, even *Text2Scene* [HKK23] stylizes every single object in a room, the basic rule of view planning is to make cameras face the object. A common criterion is to (randomly) sample around predefined principal cameras or along the camera trajectory. Data augmentation is a common trick as well, such as random perspective transformation and random resize plus crop [MBOL\*22, MZS\*23], rendering with random backgrounds [HKK23], mirroring and rotating subject elements for rendering [AONA22]. It is noted that *PSNet* [CWNN20] relies on a pre-trained point cloud classifier for feature extraction, thus it does not require 2D view supervision.

**3D Geometry Consistency.** Appearance-only 3D stylization requires keeping 3D geometry constant before and after stylization.

*Frozen Geometry.* The frequently used strategy is to freeze geometry during the stylization stage. For built or reconstructed 3D assets such as mesh, volume, and point clouds, stylization can occur merely on appearance properties such as texture of mesh [HJN22, RMA\*23, CSL\*23], albedo of volume [GLZ\*21], color of points [CWNN20], and point appearance transformation [HTS\*21]. When it comes to implicit reconstruction with implicit or hybrid representations such as NeRF, existing works tend to freeze the geometry branch during stylization [CTT\*22, HHY\*22, LZC\*23, CYL\*22, ZKB\*22, ZHX\*23, FJW\*22, PHY23, ZLH\*23, NPLX22, WCF\*23]. Particularly, some use hyper MLPs to predict stylized appearance branch parameters for stylization while fixing geometry branch parameters for 3D geometric consistency [CTT\*22, CYL\*22, WCF\*23].

**Multi-view Appearance Consistency.** For both geometry and appearance stylization, we need to consider both 3D geometry and multi-view appearance consistency. 3D assets with explicit appearance properties such as texture, point cloud, volume colors are multi-view appearance consistent themselves intrinsically. However, implicit representations may lead to multi-view appearance inconsistency, for example, view-dependent effects in NeRF.

*View-independent Style.* For NeRF or other variants, a brute-force way is to optimize stylized scenes without viewing direction input [ZKB\*22, ZHX\*23, LZC\*23, PHY23], discarding view dependent effects for better multi-view appearance consistency.

*Depth and Angle Awareness.* *StyleMesh* [HJN22] uses mesh surface depths and normals (angles) to leverage the weights of style optimization on each surface, coming to a 3D-aware stylization. It solves the problem of stretched and distorted artistic motifs synthesized on surfaces due to discrepancy of viewing angles in training multi-views.

*2D-to-3D Feature Lifting.* Existing novel view stylization works rely on the large-data pre-trained 2D models, and some feed-forward methods would like to lift 2D to 3D features [HTS\*21, HHY\*22,

Literature	Extra Input	Semantic Matching Technique
[MBOL*22] [MZS*23] [WCF*23]	text	Design a text prompt for local stylization.
[GAG*23]	none	Use the identity-preserving term to keep deformation not far from input mesh.
[HKK23]	mesh label	3D instance mesh label for instance-level stylization.
[LZC*23]	3D mask	Obtain 3D mask by NeRF-based object segmentation, and apply different 2D styles to masked and unmasked 3D regions.
[ZHX*23]	none	Semantic matched edited view as reference; A feature dictionary based on semantics; Propagate style features to other views via point intersection and nearest neighbor searching.
[PHY23]	seg maps	Train NeRF to obtain 3D-consistent segmentation from multi-view segmentation maps; Stylize NeRF with correspondent 3D scene and 2D style segments.
[SCD*23]	text, 3D mask	Off-the-shelf text-guided segmentation model to segment each view for semantic-aware training.

Table 3: Summary of semantic alignment in selected 3D neural stylization methods.

[LZC\*23]. Both *LSNV* [LLKY19] and *StyleRF* lift multi-view content features to the 3D scene from the pre-trained VGG. Specifically, *LSNV* [LLKY19] utilizes point clouds to project multi-view point-based features to 3D point clouds, while *StyleRF* lifts multi-view VGG feature to 3D feature grid. In the stylization stage, both use the 3D consistent content features for style transformation, though still use the per-view feature for supervision. *StylizedNeRF* [HHY\*22] trains a 2D AdaIN model with rendered consistent multi-views as content images and adopts an additional multi-view consistency loss for training, which harnesses the AdaIN model with 3D awareness.

**3D-Aware Style Feature.** Some mesh stylization works try to optimize the scene with average features among multiple views. But they only support several views for an object in each iteration (e.g., 5 views [MBOL\*22, MZS\*23]). Such a strategy of averaging features and gradients unnecessarily coherent 3D style transformation, and may lead to some artifacts such as messy and incorrect geometry. Thus, Gao *et al.* [GAG\*23] proposed multi-view patch-wise consistent loss at the CLIP feature level to regularize transformation.

### 3.7.2. Controllability

3D digital elements share diverse properties for different stylish innovations, such as shape, color, materials, and animation. This report concentrates on 3D stylization works in terms of artistic, photorealistic, semantic, geometry and appearance stylization genres.

**Control on Geometry and Appearance Stylization.** By inheriting 2D neural stylization capabilities, 3D stylization works achieve basic artistic, photorealistic and semantic stylization. In addition, the state of the art validates the flexibility of neural stylization on 3D data, which enables either 3D geometry or appearance stylization. The disentanglement of geometry and appearance controls [HKK23, KAGS20, CWNN20, WCF\*23] in 3D representations is essential for stylization regulation and restriction.

**Semantic Alignment.** Table 3 summarizes the tricks for semantic stylization in 3D data. Some approaches consider explicit semantic matching [HKK23, HHY\*22, ZHX\*23, PHY23, SCD\*23], for

example, *Text2Scene* inputs 3D labels, *Ref-NPR* [ZHX\*23] is supervised by an edited view with matched semantics, *StyleRF* [LZC\*23] uses 3D mask for multi-style composition at inference, Pang *et al.* [PHY23] supervise training by explicit segmentation maps input, *Blending-NeRF* [SCD\*23] relies on zero-shot segmentation model CLIPSeg [LE22]. Some employ implicit matching through latent feature searching, such as nearest neighbor feature matching [ZKB\*22, PHY23, ZHX\*23], although this method only reaches feature-level matching. [GAG\*23] proposed a regularization term to preserve identity. Some [MBOL\*22, MZS\*23, WCF\*23] rely on deliberate text prompts for local stylization.

### 3.7.3. Generalization

**Arbitrary Styles.** The SOTA data-driven pre-trained 3D stylization models can generalize to new styles in a zero-shot manner, for example, novel view stylization includes [HTS\*21, CTT\*22, HHY\*22, LZC\*23], and volumetric stylization includes [GLZ\*21]. Specifically, in NeRF stylization, [CYL\*22, CTT\*22, HHY\*22] train a 3D style transfer module, as known as the appearance branch, for a scene with different style features, while [HTS\*21, LZC\*23] learn feature transformation for arbitrary styles. [GLZ\*21] requires both 3D volume and 2D style datasets for training.

**Generalize to Diverse Scenes.** *LSNV* [HTS\*21] supports stylizing arbitrary scenes without retraining given posed views, point clouds, and depth maps. *SNeRF* [NPLX22] and *Instruct-NeRF2NeRF* [HTE\*23] introduce a general framework for a single scene optimization with either image or textual reference. They are applicable to any scene, any style, either geometry or appearance stylization.

### 3.7.4. Efficiency

**Fast and Photorealistic Rendering.** [MZS\*23] and [AONA22] proposed to use networks (MLP and CNN) to accelerate existing single-style optimization based mesh and volumetric stylization methods [MBOL\*22, KAGS19]. [GLZ\*21] trained a feedforward network for arbitrary style transfer for volumetric simulation and achieved efficient inference speed.

Implicit scenes tend to utilize explicit 3D representations and data structures for sampling acceleration [RK21, FTC\*22, SSC22, MESK22, TWN\*23], and some apply low-rank tensor feature multiplication for memory efficiency [CXG\*22]. Table 4 features novel view stylization methods with applied base reconstruction techniques. Most works tend to employ currently developed quick reconstruction and rendering techniques for fast stylization, but applicable scene scale is limited due to data structure such as voxel grids.

**Rendering and Back-propagation.** In NeRF stylization, naive NeRF-based rendering is memory-intensive for a bulk of ray samplings and point queries, but style losses are based on full images. Therefore, some proposed patch-based training [CTT\*22], deferred gradient back-propagation [ZKB\*22], and some separate forward and back-forward steps with full-res computation and patch-wise back-propagation [ZLH\*23, WJC\*23, WCF\*23].

## 4. Datasets and Evaluation for 3D Stylization

In this section, we summarize the frequently used datasets for 3D neural stylization and provide a mini-benchmark on 3D artistic stylization as a reference for future works.

Literature	Base Tech.	Data Struct.	Scale <sup>a</sup>	Rendering <sup>b</sup>
[HTS*21]	FVS [RK20], LST [LLKY19]	point cloud	large	<1s
[CTT*22]	NeRF++ [ZRSK20], HyperNet [HDL16]	N/A	large	>1s
[HHY*22]	NeRF [MST*20], AdaIN [HB17]	N/A	any	>1s
[FJW*22]	NeRF [MST*20], Gatys <i>et al.</i> [GEB16]	N/A	small	>1s
[ZKB*22]	Plenoxels [FTC*22], NNFM	grid	small	<1s
[CYL*22]	DVGO [SSC22], I2I-GAN	grid	small	<1s
[NPLX22]	any NeRF, any NST	N/A	any	depends
[WJC*23]	VolSDF [YGKL21], CLIP [RKH*21]	N/A	small	<1s
[LZC*23]	TensoRF [CXG*22], LST [LLKY19]	grid	small	<1s
[ZLH*23]	Plenoxels [FTC*22]	grid	small	<1s
[ZHX*23]	Plenoxels [FTC*22], NNFM [ZKB*22]	grid	small	<1s
[PHY23]	InstantNGP [MESK22], NNFM [ZKB*22]	hash grid	medium	<1s
[HTE*23]	NeRFacto [TWN*23], InstructP2P [BHE23]	hash	any	depends
[SCD*23]	NeRF [MST*20], CLIP [RKH*21]	N/A	small	>1s

<sup>a</sup>Scale refers to scene scale, small as objects, medium as a forward-facing scene, large as unbounded scenes.

<sup>b</sup>Rendering time per image of  $256 \times 256$  at inference.

Table 4: Summary of selected novel view stylization methods in terms of the base techniques of 3D reconstruction and neural stylization. Displayed in chronological order.

ization as a reference for future works. We first summarize popular 3D datasets and style reference images for 3D stylization. Next, we introduce existing evaluation metrics and criteria for 2D and 3D stylization, and some deprecated 2D baselines for 3D stylization tasks. Finally, we conducted evaluation experiments on novel view stylization across different scales of scenes and introduce a mini-benchmark for artistic novel view stylization.

### 4.1. Datasets

Datasets are essential for validating performance of 3D stylization in terms of applicable scenarios, stylization diversity, etc. Table 5 illustrates selected popular 3D and 2D datasets for the evaluation of 3D neural stylization works, including datasets of mesh, point cloud, novel view synthesis, and style reference images.

### 4.2. Evaluation Criteria and Metrics

We derive several critical aspects from the state-of-the-art 3D neural stylization works for evaluating 3D stylization performance.

**Similarity.** Stylization aims to stylize a subject with a similar geometry but the target style. PSNR, SSIM and LPIPS [ZIE\*18] are popular metrics for reconstruction evaluation as well as measuring structure and appearance similarity.

**Semantic Matching.** A number of 2D neural style transfer methods [CVS\*22, TBTBD22] have adopted semantic segmentation to different extents for better chrominance matching and 2D geometry preservation. Recent 3D neural stylization techniques, especially prompt-driven ones, also managed to achieve semantic matching (Table 3). Visual metrics such as intersection over union (IoU) and average precision (AP) are popular in scene segmentation understanding. Prompt-based metrics can rely on CLIP [RKH\*21], which provides access to semantic control via language prompts, and text-image



	Dataset Name	Content	#Scenes/Images	Synthetic or Real	Highlights
Mesh	TurboSquid [tur23]	(textured) mesh model	N/A	synthetic	Professional publicly shared 3D models
	CGTrader [cgt23]	(textured) mesh model	1.81M	synthetic	Professional publicly shared 3D models
	ShapeNet [CFG*15]	mesh model	3M	synthetic	Annotated 3D CAD object models
	COSEG [SVKK*11]	mesh model	172	synthetic	Shapes with segment annotations
	ModelNet [WSK*15]	mesh model	151,128	synthetic	3D CAD object models
	Thing10K [ZJ16]	mesh model	10K	synthetic	3D-printing models
	Objaverse 1.0 [DSS*23]	(textured) mesh model	10M	synthetic	Annotated 3D objects and scenes sourced from Sketchfab
Pt.	DensePoint [CN19]	colored point cloud	10,454	synthetic	Point clouds built on ShapeNet and ShapeNetPart [YKC*16]
Novel View Synthesis	DTU (MVS) [JDV*14]	multi-views, MVS	124	real	Scanned objects
	LLFF [MSOC*19]	multi-views	24	real	Forward-facing scenes
	NeRF-Real [MST*20]	multi-views	2	real	Centered objects with background 360° images
	NeRF-Synthetic [MST*20]	posed multi-views	8	synthetic	Centered objects w/o background 360° images rendered by Blender
	Tanks and Temples (TnT) [KPZK17]	multi-views	21	real	Large indoor and outdoor scenes
	Real Lego [FTC*22]	multi-views	1	real	Centered Lego with background 360° images
	Mip-NeRF 360 [BMV*22a]	multi-views	9	real	Inward-facing object-centric 360° indoor and outdoor scenes
Style Image <sup>o</sup>	Painter by Numbers (WikiArt) [kag16]	painting	79,433/23,815	Real	Artistic paintings from WikiArt
	DPST [LPSB17]	photo	60	Real	Photorealistic stylish photos
	COCO [LMB*14]	photo	83K/41K	Real	Large-scale objects in context

Table 5: Popular datasets for performance evaluation on 3D neural stylization. Pt. is the abbreviation of point cloud. <sup>a</sup> Train/Test sets.

similarity computation scheme (i.e., Eq. 4 and 5). For example, *Instruct-NeRF2NeRF* [HTE\*23] conducted CLIP text-image direction similarity [GPM\*22] and a novel temporal CLIP direction consistency score for evaluation. *X-Mesh* [MZS\*23] introduced **MES** that takes both text-image conformity and multi-view consistency into consideration, which calculates the average of cosine similarity between 24 uniformly sampled views and the target prompt.

**Multi-view Consistency.** 3D representations inherently provide multi-view geometry consistency. To measure multi-view appearance consistency, some 3D stylization works refer to video temporal short-range and long-range consistency evaluation [LHW\*18] using warping difference error [CTT\*22, LZC\*23, ZLH\*23, NPLX22, HJN22] and the warped LPIPS [HTS\*21, CYL\*22, HHY\*22, LZC\*23, WCF\*23], via optical flow estimation [CTT\*22, LZC\*23, ZLH\*23, NPLX22, CYL\*22] or camera and depth/geometry estimation [HTS\*21, HHY\*22, HJN22]. *Ref-NPR* [ZHx\*23] also adopts LPIPS to measure consistency between the edited reference view and its 10 nearest test views similar to CCPL [WZDB22]. As mentioned in semantic matching, CLIP can be applied in multi-view semantic consistency evaluation [HTE\*23, MZS\*23].

**Visual Quality.** For image synthesis, we expect synthesized images to look natural and contain as few artifacts as possible. The inception score (IS) [SGZ\*16] is designed to measure the image quality and diversity of generated images. An image will be considered high-quality if a pre-trained classification model gives it a low entropy. Another popular metric is Frchet Inception Distance (FID) [HRU\*17], which compares the distribution of generated images with the distribution of real images. It works well to decide if generated images are similar to objects in the target domain. For instance, *TSNeRF* [WCF\*23] used FID to evaluate the distance between stylized rendered views and target art database. IS and FID are widely adopted in generative image-to-image translation models [HLBK18, LHM\*19, CVS\*22].

**Robustness and Efficiency.** For model robustness, *Ref-NPR* [ZHx\*23] measured PSNR along a camera trajectory between renderings of stylized NeRF  $w_{NP}$  given user edited view and other stylized NeRFs given other rendered view by  $w_{NP}$  as reference. It is not essential for general 3D neural stylization evaluation, but it can be taken as a reference. As for the training and inference efficiency, current methods can be classified into different types in terms of data requirement, training time and rendering speed (see Table 1). Recently, *X-Mesh* [MZS\*23] introduced **ITS** to evaluate the convergence rate of the model. The number of iterations needed to reach the target MES represents the training efficiency. Hopefully, the idea may evolve into a standard metric for the evaluation of future 3D neural stylization methods.

**User Study.** While the above metrics can somehow evaluate 3D stylization performance, it goes beyond standard evaluation metrics on some non-trivial cases such as subjectively judging the naturalness and visual artifacts for generated scenes. Therefore, involvement of user study is a suitable choice. A typical user study involves the following steps: participant recruitment, user study materials and questionnaire preparation, answer collection, and statistic analysis. The performance of "stylization quality", and "temporal consistency" are most frequently evaluated in 3D stylization [HTS\*21, CTT\*22, CYL\*22, LZC\*23].

### 4.3. Baselines

Before the advent of sufficient 3D stylization works, 2D image and video neural stylization methods were commonly used as baselines in 3D stylization evaluation.

**2D Neural Stylization.** Image style transfer baselines involve artistic style transfer methods, such as AdaIN [HB17] and LST [LDMG\*17], and photorealistic style transfer methods, such as WCT<sup>2</sup> [YUC\*19] and CCPL [WZDB22]. With temporal consistency, video stylization baselines include MCC [DTD\*21],

FMVST [GLYY20], CompoundVST [WXZ\*20], CCPL [WZDB22], ReReVST [WYXL20].

**2D Stylization plus Novel View Synthesis.** As a relatively new problem of novel view stylization, some reference pipelines combine 2D stylization approach and novel view synthesis [HTS\*21]:

- Image stylization → novel view synthesis.
- Novel view synthesis → image stylization.
- Novel view synthesis → video stylization.

Though 2D baselines can achieve stylized views, 3D stylization works [HTS\*21, CTT\*22, HHY\*22] have demonstrated 3D neural stylization approaches are superior to these multi-view inconsistent 2D baselines in terms of 3D geometric and appearance consistency.

#### 4.4. Mini-benchmark of 3D Artistic Stylization

Artistic stylization for implicit scenes is mostly developed among the reviewed state of the art. In this section, we evaluated state-of-the-art 3D stylization generative models [HTS\*21, CTT\*22, HHY\*22, LZC\*23] and single-style per-scene stylization works [ZKB\*22, FJW\*22, NPLX22, ZHX\*23, WJC\*23, HTE\*23] over eight scenes from three public datasets, including object scenes (chair, mic) in NeRF-Synthetic [MST\*20] that are inward-facing 360° objects without background, forward-facing real scenes (fern, flower, horns, trex) in LLFF dataset [MSOC\*19], and large unbounded real scenes (Truck, Playground) in Tanks and Temples dataset [KPZK17]. Particularly, masked large scenes Caterpillar and Truck without background [KPZK17] are instead used for StyleRF and INS.

We evaluated multi-view consistency and style similarity for each artistic novel view stylization method, and visual quality using FID and KID for some arbitrary style transfer models [HTS\*21, CTT\*22, LZC\*23]. We followed multi-view consistency evaluation pipelines [HTS\*21, NPLX22, LZC\*23, ZHX\*23], and evaluated short-range and long-range warp error with MSE and LPIPS scores. For style similarity, we computed VGG feature Gram matrix style loss (Eq. 3) as a metric. Specifically, we rendered a short sequence of novel views around each scene and computed the similarity of adjacent frames for short-range score and far-away frames (e.g., 10-frame interval) for long-range score. Similar to [LHW\*18], we warped each original frame to another target frame via off-the-shelf optical flow estimator RAFT [TD20] and computed the occlusion mask on frames before stylization, then calculated mean square error (MSE) [LHW\*18] and LPIPS [HHY\*22, LZC\*23] on the overlapped area of frames after stylization as cross-view similarity metrics. Only pixels or features located in non-occluded mask areas are taken into account. We used existing official implementations of methods, and edited reference views by AdaIN for *Ref-NPR*. We reproduced *SNeRF* based on Plenoxels (fixed geometry) similar to [ZKB\*22, ZHX\*23, ZLH\*23], and Gatys *et al.* [GEB16] (named SNeRF-G) or the pre-trained AdaIN model (named SNeRF-A) with 5 training iterations. 120 WikiArt style references are used for FID and KID, and 6 WikiArt images for warp error and style loss. All experiments were conducted on GeForce RTX 3090 GPUs with 24GB memory per GPU.

##### 4.4.1. Evaluation Results

Tables 6 reports the short-range and long-range consistency and style loss (Gram loss), Table 7 shows FID and KID metrics for style

	Method	Object		Forward-face		Large Scene		Average	
		MSE	LPIPS	MSE	LPIPS	MSE	LPIPS	MSE	LPIPS
Short-range Warp Error↓	LSNV	0.0396	0.0999	0.0146	0.0701	0.0198	0.0818	0.0222	0.0805
	HyperStyle	<b>0.0067</b>	<b>0.0320</b>	0.0125	0.0778	0.0083	0.0482	0.0104	0.0628
	StyleRF	0.0086	0.0513	0.0095	0.0517	0.0134 <sup>c</sup>	0.0620 <sup>c</sup>	0.0102	0.0542
	ARF	0.0255	0.0508	0.0084	0.0515	0.0081	0.0356	0.0128	0.0460
	Ref-NPR <sup>b</sup>	0.0191	0.0580	0.0072	0.0594	0.0062	0.0353	0.0100	0.0530
	INS	0.0293	0.0343	0.0135	0.0534	0.0786 <sup>c</sup>	0.1837 <sup>c</sup>	0.0337	0.0812
	SNeRF-G <sup>a</sup>	0.0230	0.0513	0.0072	0.0510	0.0060	0.0314	0.0109	0.0462
	SNeRF-A <sup>a</sup>	0.0116	0.0412	<b>0.0061</b>	<b>0.0485</b>	<b>0.0059</b>	<b>0.0312</b>	<b>0.0074</b>	<b>0.0423</b>
Long-range Warp Error↓	LSNV	0.0469	0.0983	0.0285	0.0812	0.0387	0.0928	0.0399	0.0884
	HyperStyle	<b>0.0072</b>	<b>0.0372</b>	0.0641	0.1736	<b>0.0092</b>	<b>0.0274</b>	0.0403	0.1123
	StyleRF	0.0131	0.0513	0.0181	<b>0.0681</b>	0.0216 <sup>c</sup>	0.0573 <sup>c</sup>	<b>0.0177</b>	<b>0.0612</b>
	ARF	0.0483	0.0756	0.0214	0.0927	0.0185	0.0573	0.0276	0.0752
	Ref-NPR <sup>b</sup>	0.0373	0.0767	<b>0.0178</b>	0.0968	0.0127	0.0507	0.0214	0.0802
	INS	0.0536	0.0480	0.0401	0.0944	0.1127 <sup>c</sup>	0.2092 <sup>c</sup>	0.0616	0.1115
	SNeRF-G <sup>a</sup>	0.0517	0.0835	0.0515	0.1542	0.0224	0.0768	0.0443	0.1172
	SNeRF-A <sup>a</sup>	0.0331	0.0720	0.0584	0.1790	0.0220	0.0815	0.0430	0.1278

	Method	Object	Forward-face	Large Scene	Average
Style Loss ( $\times 1e-5$ )↓	LSNV	5.3345	12.2748	6.4795	9.0909
	HyperStyle	6.3470	5.0541	5.6637	5.4130
	StyleRF	<b>4.0249</b>	4.4604	6.4243 <sup>c</sup>	4.8425
	ARF	6.7117	4.8248	8.6629	6.2468
	Ref-NPR <sup>b</sup>	6.3605	3.0653	5.4008	4.4730
	INS	5.3055	3.7685	6.2595 <sup>c</sup>	4.7755
	SNeRF-G <sup>a</sup>	5.6361	<b>1.6660</b>	<b>3.5188</b>	<b>3.1217</b>
	SNeRF-A <sup>a</sup>	6.5625	2.9703	4.4199	4.2308

<sup>a</sup>SNeRF is reproduced by Plenoxels (fixed geometry), and Gatys *et al.* (SNeRF-G) or AdaIN (SNeRF-A).

<sup>b</sup>Ref-NPR with the stylized reference view by AdaIN.

<sup>c</sup>Trained without background.

Table 6: Evaluation results for short-range and long-range consistency, and style loss.

Method	FID↓	KID↓
LSNV	<b>247.29</b>	0.044
HyperStyle	289.29	0.076
StyleRF	267.112	<b>0.043</b>

Table 7: Evaluation results of 3D arbitrary style transfer in terms of FID, KID.

diversity of stylized images generated by pre-trained 3D arbitrary style transfer models. Figure 15 displays some visual results among 3D arbitrary style and single style transfer methods.

**Multi-view Consistency.** Thanks to the implicit feature representation of scenes for novel view synthesis, all evaluated works can achieve short-range consistency. It indicates the implicit features offer a slight ability for close-view interpolation with appearance consistency. As for long-range consistency, as discussed in Section 3.7.1, discarding view-dependent effects and 2D-to-3D feature lifting help with 3D consistency. Some works prefer to preserve view-dependent

effect with viewing direction input [HDL16, FJW\*22, WCF\*23] while some prefer to discard view-dependent effect for multi-view consistency [ZKB\*22, ZHX\*23, LZC\*23]. Since supervision under multiple independent stylized views is not inherently consistent, the performance on long-range multi-view consistency metrics would be worse (e.g., Warp Error for *INS* and *SNeRF*). *StyleRF* learns 3D consistent latent features by feature lifting and *Ref-NPR* maps deterministic 2D to 3D features, and they both discard view-dependent effects, therefore they can achieve stable either short-range or long-range multi-view consistency. It is noted that *HyperStyle* [CTT\*22] tends to generate blurry novel views, which leads to good multi-view consistency scores.

**Performance in Different Scene Scales.** Based on different reconstruction approaches, 3D stylization performance may vary among scene scales. For example, *LSNV* [HTS\*21] and *HyperStyle* [CTT\*22] are more robust on unbounded scene stylization, while grid-based approaches tend to be unstable or unsuccessful for large unbounded scenes, such as *INS* [FJW\*22] and *StyleRF* [LZC\*23].

**Performance in Style Coherency.** By assessing style loss between stylized views and target style references (see style loss in Table 6), in general, single style optimization approaches [ZKB\*22, ZHX\*23, WCF\*23] obtain closer style features to the given target style reference than arbitrary style transfer models [HTS\*21, CTT\*22, LZC\*23]. From visual results in Figure 15, single style optimization methods *ARF* and *SNeRF* successfully learned correct brushstrokes and subtle motifs from reference paintings, while arbitrary style transfer models *StyleRF* and *LSNV* tend to generate harsher patterns with thicker brushstrokes.

**Challenge in Text-guided 3D Artistic Stylization.** In our experience with stylizing scenes with text prompts for artistic styles, we found that some text-guided optimization methods such as *Instruct-NeRF2NeRF* [HTE\*23] cannot handle abstract artistic style description, which leads to dramatic geometry destruction. For example, "Vincent van Gogh" stylization using the text prompt does not work because *Instruct-Pix2Pix* [BHE23] on multi-view images gets too much geometric inconsistency with artistic abstract patterns, which degrades the NeRF optimization. To achieve abstract style transfer for 3D scenes, additional datasets for fine-tuning feature extractors may be necessary such as *TSNeRF* [WCF\*23].

## 5. Open Challenges and Future Work

From this survey, we identify under-explored problems and notable challenges in 3D neural stylization that are worth investigating in future work, which we discuss below.

**Limitation in Scene Scale.** All state-of-the-art works for 3D neural stylization support basically as small as objects, object-centric scenes, and up to room scale, and outdoor inward-facing scenes. 3D assets and scenes can scale to as large as multi-room indoor scene [SWM\*19, HCZY22, BMV\*23], architectural scenes [JMM\*20, MBRs\*21, WWG\*21], multi-block outdoor scenes [TCY\*22, TZFR23], and even city-scale scenes [XXP\*22, XXP\*23, LJX\*23]. These complex scenarios with intricate semantics are challenging for stylization and semantic alignments.

**Generalization to Different Scene Classes.** To the best of our

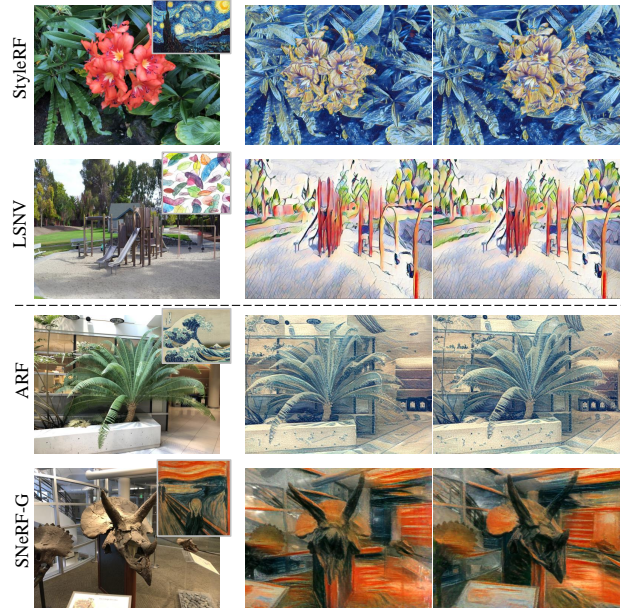


Figure 15: Novel view stylization results. Zoom in for details.

knowledge, few of the works [HTS\*21, FWY\*23] achieve generic scene stylization in one model. Pre-trained 2D arbitrary style transfer models [HB17, LLKY19] support stylizing any scene with any target style. It has the potential to develop a 3D stylization model for general scenes, for example, based on advanced generalizable NeRF variants without or with little fine-tuning [WWG\*21, LPL\*22, JLF22, HZF\*23].

**Generalizable Text-guided Stylization.** Text-guided 3D scene stylization and editing are still in the early stages. Data-driven generalizable text-guided 3D scene stylization or editing is seldom explored yet [FWY\*23], which demands more attention. It is worth investigation and explorability, since current advanced large-language models such as BLIP [LLSH23], GPT [BMR\*20] enable infinite image-text pair data generation for data-driven model training.

**3D-Holistic Style Feature.** This report summarizes 3D neural stylization works mainly based on large-data 2D pixel-level feature extractors, since large-data 3D pre-trained models are still rare and expensive. Even though some works [HTS\*21, LZC\*23] try to lift 2D content features to 3D before 3D stylization (Section 3.7.1), they still use view-dependent style features for final 3D stylization supervision. It is also impractical to lift 2D features to 3D at every iteration. Some works [MBOL\*22, MZS\*23] supervise stylization with a 3D-aware style feature by averaging features of several views for a small object (Section 3.7.1), which is not implementable for more views with limited memory. Per-view or multi-view supervision may not be sufficient to represent the whole 3D scene style feature, and worse may dilute the current single-view style from other views with conflicting gradients [GAG\*23]. More research and investigation is needed for efficient 3D-aware and even 3D-holistic style feature for 3D stylization.

**Diversity of Stylization Genres.** This report discussed a few styliza-



tion genres such as artistic, semantic, and photorealistic stylization. There remain stylization methods that are left beyond these genres such as stylization from physical scene modeling such as material editing, illumination changes, etc. Although there are some works on decomposing 3D scenes for material stylization [LZJ\*22] and relighting [BBJ\*21, SDZ\*21, ZSD\*21, BJB\*21, LSB\*22], their stylization results, controllability, and rendering quality remain in an exploratory stage.

**Standardized Evaluation on Other Stylization Problems.** We provided only a mini-benchmark for artistic novel view stylization, while other 3D stylization tasks are still developing evaluation criteria except for user study. We believe there should be some variations from the evaluation of our mini-benchmark, for other 3D stylization problems, while concerns should be similar (Section 4.2).

**Potential Applications and Industrial Production.** 3D neural stylization provides automatic stylization techniques for 3D assets including mesh, point cloud, volumetric simulation, and novel views. Stylized assets can be seamlessly integrated into traditional computer graphics rendering pipelines and software, such as meshes with new stylized texture, re-colored point clouds, and stylized volumetric simulation. Implicit reconstructed scenes, such as NeRF, can be exported as textured mesh or rendered by game engine plugins such as Luma AI’s Unreal Engine NeRF plug-ins [Lum23]. Automated 3D environment synthesis holds great promise for film production and virtual production applications. For instance, combining environmental NeRF with light stages [Man23] enables cost-effective scene shooting using Volinga suite [Vol23]. Non-photorealistic stylized 3D scenes are particularly beneficial for animation production, as demonstrated by the film *Elemental* [HHK\*23, KAOT23]. Moreover, these techniques find possible applications in VR and video game development [MLS\*22], enabling rapid stylization and editing of 3D scenes [LZC\*23, FWY\*23].

## 6. Conclusion

The state of the art report has explored the advancements in 3D neural stylization, especially image- and text-guided neural stylization techniques for 3D data. Through this comprehensive survey of recent 3D neural stylization techniques and corresponding applications, we highlighted the importance of neural stylization in accelerating the creative process, enabling fine-grained control over stylization, and enhancing artistic expression in various domains such as movie making, virtual production, and video game development. Furthermore, we have introduced a taxonomy for neural stylization, providing a framework for categorizing new works in the neural stylization field. Our analysis and discussion of advanced techniques underscored the ongoing research efforts aimed at addressing limitations and pushing the boundaries of neural stylization in 3D digital domain. Finally, we proposed a mini-benchmark of 3D artistic stylization, which we aim to offer inspiration and a standard of evaluation for other 3D stylization works.

## References

[Aar18] AARON H.: Image stylization: History and future (part 1), Jun 2018. Accessed on 15 June 2022. URL: <https://research.adobe.com/news/image-stylization-history-and-future/>. 6

[AGK\*22] AIGERMAN N., GUPTA K., KIM V. G., CHAUDHURI S., SAITO J., GROUEIX T.: Neural jacobian fields: Learning intrinsic mappings of arbitrary meshes. *ACM Transactions on Graphics* 41, 4 (jul 2022). doi:10.1145/3528223.3530141. 9, 10

[AONA22] AURAND J., ORTIZ R., NAUER S., AZEVEDO V. C.: Efficient neural style transfer for volumetric simulations. *ACM Transactions on Graphics (TOG)* 41, 6 (2022), 1–10. 8, 9, 11, 14, 15, 16

[BBJ\*21] BOSS M., BRAUN R., JAMPANI V., BARRON J. T., LIU C., LENSCH H.: Nerd: Neural reflectance decomposition from image collections. In *Proceedings of the IEEE/CVF International Conference on Computer Vision* (2021), pp. 12684–12694. 20

[BHE23] BROOKS T., HOLYNSKI A., EFROS A. A.: Instructpix2pix: Learning to follow image editing instructions. In *Proceedings of the IEEE/CVF Conference on Computer Vision and Pattern Recognition* (2023), pp. 18392–18402. 6, 12, 16, 19

[BJB\*21] BOSS M., JAMPANI V., BRAUN R., LIU C., BARRON J., LENSCH H.: Neural-pil: Neural pre-integrated lighting for reflectance decomposition. *Advances in Neural Information Processing Systems* 34 (2021), 10691–10704. 20

[BMR\*20] BROWN T., MANN B., RYDER N., SUBBIAH M., KAPLAN J. D., DHARIWAL P., NEELAKANTAN A., SHYAM P., SASTRY G., ASKELL A., ET AL.: Language models are few-shot learners. *Advances in neural information processing systems* 33 (2020), 1877–1901. 6, 19

[BMV\*22a] BARRON J. T., MILDENHALL B., VERBIN D., SRINIVASAN P. P., HEDMAN P.: Mip-nerf 360: Unbounded anti-aliased neural radiance fields. In *Proceedings of the IEEE/CVF Conference on Computer Vision and Pattern Recognition* (2022), pp. 5470–5479. 7, 13, 17

[BMV\*22b] BARRON J. T., MILDENHALL B., VERBIN D., SRINIVASAN P. P., HEDMAN P.: Mip-nerf 360: Unbounded anti-aliased neural radiance fields. *CVPR* (2022). 7

[BMV\*23] BARRON J. T., MILDENHALL B., VERBIN D., SRINIVASAN P. P., HEDMAN P.: Zip-nerf: Anti-aliased grid-based neural radiance fields. *Proceedings of the IEEE/CVF International Conference on Computer Vision* (2023). 7, 19

[BSSE21] BATZOLIS G., STANCZUK J., SCHÖNLIEB C.-B., ETMANN C.: Conditional image generation with score-based diffusion models. *arXiv preprint arXiv:2111.13606* (2021). 5

[BZY\*23] BAO C., ZHANG Y., YANG B., FAN T., YANG Z., BAO H., ZHANG G., CUI Z.: Sine: Semantic-driven image-based nerf editing with prior-guided editing field. In *The IEEE/CVF Computer Vision and Pattern Recognition Conference (CVPR)* (2023). 13

[CCJJ23] CHEN R., CHEN Y., JIAO N., JIA K.: Fantasia3d: Disentangling geometry and appearance for high-quality text-to-3d content creation. In *Proceedings of the IEEE/CVF International Conference on Computer Vision (ICCV)* (October 2023). 10

[CFG\*15] CHANG A. X., FUNKHOUSER T., GUIBAS L., HANRAHAN P., HUANG Q., LI Z., SAVARESE S., SAVVA M., SONG S., SU H., XIAO J., YI L., YU F.: *ShapeNet: An Information-Rich 3D Model Repository*. Tech. Rep. arXiv:1512.03012 [cs.GR], Stanford University - Princeton University - Toyota Technological Institute at Chicago, 2015. 17

[CFHT23] CHEN Z., FUNKHOUSER T., HEDMAN P., TAGLIASACCHI A.: Mobilenerf: Exploiting the polygon rasterization pipeline for efficient neural field rendering on mobile architectures. In *Proceedings of the IEEE/CVF Conference on Computer Vision and Pattern Recognition* (2023), pp. 16569–16578. 6, 7

[cgt23] Cgtrader, 2023. URL: <https://www.cgtrader.com/>. 17

[CKNH20] CHEN T., KORNBLITH S., NOROUZI M., HINTON G.: A simple framework for contrastive learning of visual representations. In *International conference on machine learning* (2020), PMLR, pp. 1597–1607. 13

[CN19] CAO X., NAGAO K.: Point cloud colorization based on densely annotated 3d shape dataset. In *Multimedia Modeling: 25th International Conference, MMM 2019, Thessaloniki, Greece, January 8–11, 2019, Proceedings, Part I* 25 (2019), Springer, pp. 436–446. 17



- [CSL\*23] CHEN D. Z., SIDDIQUI Y., LEE H.-Y., TULYAKOV S., NIESSNER M.: Text2tex: Text-driven texture synthesis via diffusion models. In *Proceedings of the IEEE/CVF International Conference on Computer Vision (ICCV)* (2023). 8, 9, 10, 14, 15
- [CTT\*22] CHIANG P.-Z., TSAI M.-S., TSENG H.-Y., LAI W.-S., CHIU W.-C.: Stylizing 3d scene via implicit representation and hypernetwork. In *Proceedings of the IEEE/CVF Winter Conference on Applications of Computer Vision* (2022), pp. 1475–1484. 8, 9, 12, 13, 14, 15, 16, 17, 18, 19
- [CVS\*22] CHEN Y., VU T.-A., SHUM K.-C., YEUNG S.-K., HUA B.-S.: Time-of-day neural style transfer for architectural photographs. In *2022 IEEE International Conference on Computational Photography (ICCP)* (2022), IEEE, pp. 1–12. 5, 16, 17
- [CWC20] CHANG H.-Y., WANG Z., CHUANG Y.-Y.: Domain-specific mappings for generative adversarial style transfer. In *European Conference on Computer Vision* (2020), Springer, pp. 573–589. 5
- [CWNN20] CAO X., WANG W., NAGAO K., NAKAMURA R.: Psnnet: A style transfer network for point cloud stylization on geometry and color. In *Proceedings of the IEEE/CVF Winter Conference on Applications of Computer Vision* (2020), pp. 3337–3345. 1, 8, 9, 11, 15
- [CWZ\*21] CHEN H., WANG Z., ZHANG H., ZUO Z., LI A., XING W., LU D., ET AL.: Artistic style transfer with internal-external learning and contrastive learning. *Advances in Neural Information Processing Systems* 34 (2021), 26561–26573. 4
- [CXG\*22] CHEN A., XU Z., GEIGER A., YU J., SU H.: Tensorf: Tensorial radiance fields. In *European Conference on Computer Vision* (2022), Springer, pp. 333–350. 7, 12, 14, 16
- [CYL\*18] CHEN D., YUAN L., LIAO J., YU N., HUA G.: Stereoscopic neural style transfer. In *Proceedings of the IEEE Conference on Computer Vision and Pattern Recognition* (2018), pp. 6654–6663. 11
- [CYL\*22] CHEN Y., YUAN Q., LI Z., LIU Y., WANG W., XIE C., WEN X., YU Q.: Upst-nerf: Universal photorealistic style transfer of neural radiance fields for 3d scene. *arXiv preprint arXiv:2208.07059* (2022). 8, 9, 12, 14, 15, 16, 17
- [CZG\*21] CHANDRAN P., ZOISS G., GOTARDO P., GROSS M., BRADLEY D.: Adaptive convolutions for structure-aware style transfer. In *Proceedings of the IEEE/CVF conference on computer vision and pattern recognition* (2021), pp. 7972–7981. 4
- [DDS\*09] DENG J., DONG W., SOCHER R., LI L.-J., LI K., FEI-FEI L.: Imagenet: A large-scale hierarchical image database. In *2009 IEEE conference on computer vision and pattern recognition* (2009), Ieee, pp. 248–255. 2
- [DN21] DHARIWAL P., NICHOL A.: Diffusion models beat gans on image synthesis. *Advances in neural information processing systems* 34 (2021), 8780–8794. 5
- [DSK17] DUMOULIN V., SHLENS J., KUDLUR M.: A learned representation for artistic style. In *International Conference on Learning Representations* (2017). 3, 4
- [DSS\*23] DEITKE M., SCHWENK D., SALVADOR J., WEIHS L., MICHEL O., VANDERBILT E., SCHMIDT L., EHSANI K., KEMBHAVI A., FARHADI A.: Objaverse: A universe of annotated 3d objects. In *Proceedings of the IEEE/CVF Conference on Computer Vision and Pattern Recognition* (2023), pp. 13142–13153. 17
- [DTD\*21] DENG Y., TANG F., DONG W., HUANG H., MA C., XU C.: Arbitrary video style transfer via multi-channel correlation. In *Proceedings of the AAAI Conference on Artificial Intelligence* (2021), pp. 1210–1217. 17
- [EF01] EFROS A. A., FREEMAN W. T.: Image quilting for texture synthesis and transfer. In *Proceedings of the 28th annual conference on Computer graphics and interactive techniques* (2001), pp. 341–346. 6
- [FJW\*22] FAN Z., JIANG Y., WANG P., GONG X., XU D., WANG Z.: Unified implicit neural stylization. In *European Conference on Computer Vision* (2022), Springer, pp. 636–654. 8, 9, 11, 12, 13, 15, 16, 18, 19
- [FTC\*22] FRIDOVICH-KEIL S. AND YU A., TANCIK M., CHEN Q., RECHT B., KANAZAWA A.: Plenoxels: Radiance fields without neural networks. In *Proceedings of the IEEE/CVF Conference on Computer Vision and Pattern Recognition* (2022). 6, 7, 11, 12, 13, 16, 17
- [FWY\*23] FANG S., WANG Y., YANG Y., TSAI Y.-H., DING W., YANG M.-H., ZHOU S.: Text-driven editing of 3d scenes without retraining. *arXiv preprint arXiv:2309.04917* (2023). 19, 20
- [GAG\*23] GAO W., AIGERMAN N., GROUEIX T., KIM V., HANOCKA R.: Textdeformer: Geometry manipulation using text guidance. In *ACM SIGGRAPH 2023 Conference Proceedings* (2023), pp. 1–11. 8, 9, 10, 15, 16, 19
- [GC22] GULAJEVA V., CANET M.: Psychedelic forms, 2022. URL: <https://var-mar.info/psychedelic-forms/>. 2
- [GEB16] GATYS L. A., ECKER A. S., BETHGE M.: Image style transfer using convolutional neural networks. In *Proceedings of the IEEE conference on computer vision and pattern recognition* (2016), pp. 2414–2423. 2, 3, 5, 8, 10, 11, 12, 13, 16, 18
- [GG01] GOOCH B., GOOCH A.: *Non-photorealistic rendering*. AK Peters/CRC Press, 2001. 6
- [GGSC98] GOOCH A., GOOCH B., SHIRLEY P., COHEN E.: A non-photorealistic lighting model for automatic technical illustration. In *Proceedings of the 25th annual conference on Computer graphics and interactive techniques* (1998), pp. 447–452. 6
- [GHM\*18] GONG X., HUANG H., MA L., SHEN F., LIU W., ZHANG T.: Neural stereoscopic image style transfer. In *Proceedings of the European Conference on Computer Vision (ECCV)* (2018), pp. 54–69. 11
- [GLYY20] GAO W., LI Y., YIN Y., YANG M.-H.: Fast video multi-style transfer. In *Proceedings of the IEEE/CVF winter conference on applications of computer vision* (2020), pp. 3222–3230. 18
- [GLZ\*21] GUO J., LI M., ZONG Z., LIU Y., HE J., GUO Y., YAN L.-Q.: Volumetric appearance stylization with stylizing kernel prediction network. *ACM Transactions on Graphics (TOG)* 40, 4 (2021), 162–1. 8, 9, 11, 14, 15, 16
- [GPAM\*14] GOODFELLOW I., POUGET-ABADIE J., MIRZA M., XU B., WARDE-FARLEY D., OZAIR S., COURVILLE A., BENGIO Y.: Generative adversarial nets. *Advances in neural information processing systems* 27 (2014). 5
- [GPM\*22] GAL R., PATASHNIK O., MARON H., BERMANO A. H., CHECHIK G., COHEN-OR D.: Stylegan-nada: Clip-guided domain adaptation of image generators. *ACM Transactions on Graphics (TOG)* 41, 4 (2022), 1–13. 3, 13, 17
- [Hae90] HAEBERLI P.: Paint by numbers: Abstract image representations. In *Proceedings of the 17th annual conference on Computer graphics and interactive techniques* (1990), pp. 207–214. 6
- [HB17] HUANG X., BELONGIE S.: Arbitrary style transfer in real-time with adaptive instance normalization. In *Proceedings of the IEEE international conference on computer vision* (2017), pp. 1501–1510. 3, 4, 5, 12, 14, 16, 17, 19
- [HCZY22] HUANG H., CHEN Y., ZHANG T., YEUNG S.-K.: Real-time omnidirectional roaming in large scale indoor scenes. In *SIGGRAPH Asia 2022 Technical Communications* (2022), pp. 1–5. 19
- [HDL16] HA D., DAI A., LE Q. V.: Hypernetworks. *arXiv preprint arXiv:1609.09106* (2016). 14, 16, 19
- [Her98] HERTZMANN A.: Painterly rendering with curved brush strokes of multiple sizes. In *Proceedings of the 25th annual conference on Computer graphics and interactive techniques* (1998), pp. 453–460. 6
- [HHK\*23] HOFFMAN J., HU T., KANYUK P., MARSHALL S., NGUYEN G., SCHROERS H., WITTING P.: Creating elemental characters: From sparks to fire. In *ACM SIGGRAPH 2023 Talks* (2023), pp. 1–2. 2, 6, 11, 20
- [HHY\*22] HUANG Y.-H., HE Y., YUAN Y.-J., LAI Y.-K., GAO L.: StylizedNeRF: consistent 3d scene stylization as stylized nerf via 2d-3d mutual learning. In *Proceedings of the IEEE/CVF Conference on*

- Computer Vision and Pattern Recognition* (2022), pp. 18342–18352. 8, 9, 12, 13, 14, 15, 16, 17, 18
- [HJA20] HO J., JAIN A., ABBEEL P.: Denoising diffusion probabilistic models. *Advances in neural information processing systems* 33 (2020), 6840–6851. 5
- [HJN22] HÖLLEIN L., JOHNSON J., NIESSNER M.: Stylemesh: Style transfer for indoor 3d scene reconstructions. In *Proceedings of the IEEE/CVF Conference on Computer Vision and Pattern Recognition* (2022), pp. 6198–6208. 8, 9, 10, 15, 17
- [HJO\*01] HERTZMANN A., JACOBS C. E., OLIVER N., CURLESS B., SALESIN D. H.: Image analogies. In *Proceedings of the 28th annual conference on Computer graphics and interactive techniques* (2001), pp. 327–340. 6
- [HKK23] HWANG I., KIM H., KIM Y. M.: Text2scene: Text-driven indoor scene stylization with part-aware details. In *Proceedings of the IEEE/CVF Conference on Computer Vision and Pattern Recognition* (2023), pp. 1890–1899. 8, 9, 10, 14, 15
- [HLBK18] HUANG X., LIU M.-Y., BELONGIE S., KAUTZ J.: Multimodal unsupervised image-to-image translation. In *Proceedings of the European Conference on Computer Vision (ECCV)* (2018), pp. 172–189. 5, 17
- [HMG20] HART D., MORSE B., GREENLAND J.: Style transfer for light field photography. In *Proceedings of the IEEE/CVF Winter Conference on Applications of Computer Vision* (2020), pp. 99–108. 11
- [HMT\*22] HERTZ A., MOKADY R., TENENBAUM J., ABERMAN K., PRITCH Y., COHEN-OR D.: Prompt-to-prompt image editing with cross attention control. *arXiv preprint arXiv:2208.01626* (2022). 5, 6
- [HRU\*17] HEUSEL M., RAMSAUER H., UNTERTHINER T., NESSLER B., HOCHREITER S.: Gans trained by a two time-scale update rule converge to a local nash equilibrium. *Advances in neural information processing systems* 30 (2017), 6626–6637. 17
- [HTE\*23] HAQUE A., TANCIK M., EFROS A., HOLYSKI A., KANAZAWA A.: Instruct-nerf2nerf: Editing 3d scenes with instructions. In *Proceedings of the IEEE/CVF International Conference on Computer Vision* (2023). 1, 8, 9, 11, 12, 13, 16, 17, 18, 19
- [HTS\*21] HUANG H.-P., TSENG H.-Y., SAINI S., SINGH M., YANG M.-H.: Learning to stylize novel views. In *Proceedings of the IEEE/CVF International Conference on Computer Vision* (2021), pp. 13869–13878. 8, 9, 11, 14, 15, 16, 17, 18, 19
- [HZF\*23] HUANG X., ZHANG Q., FENG Y., LI X., WANG X., WANG Q.: Local implicit ray function for generalizable radiance field representation. In *Proceedings of the IEEE/CVF Conference on Computer Vision and Pattern Recognition* (2023), pp. 97–107. 19
- [HZRS16] HE K., ZHANG X., REN S., SUN J.: Deep residual learning for image recognition. In *Proceedings of the IEEE conference on computer vision and pattern recognition* (2016), pp. 770–778. 3
- [IZZE17] ISOLA P., ZHU J.-Y., ZHOU T., EFROS A. A.: Image-to-image translation with conditional adversarial networks. In *Proceedings of the IEEE conference on computer vision and pattern recognition* (2017), pp. 1125–1134. 5
- [JAFF16] JOHNSON J., ALAHI A., FEI-FEI L.: Perceptual losses for real-time style transfer and super-resolution. In *European conference on computer vision* (2016), Springer, pp. 694–711. 3, 5, 11, 13
- [JDV\*14] JENSEN R., DAHL A., VOGIATZIS G., TOLA E., AANÆS H.: Large scale multi-view stereopsis evaluation. In *2014 IEEE Conference on Computer Vision and Pattern Recognition* (2014), IEEE, pp. 406–413. 17
- [JLF22] JOHARI M. M., LEPOITTEVIN Y., FLEURET F.: Geonerf: Generalizing nerf with geometry priors. In *Proceedings of the IEEE/CVF Conference on Computer Vision and Pattern Recognition* (2022), pp. 18365–18375. 19
- [JMM\*20] JIN Y., MISHKIN D., MISHCHUK A., MATAS J., FUA P., YI K. M., TRULLS E.: Image matching across wide baselines: From paper to practice. *International Journal of Computer Vision* (2020). 19
- [JSS17] JOSHI B., STEWART K., SHAPIRO D.: Bringing impressionism to life with neural style transfer in come swim. In *Proceedings of the ACM SIGGRAPH digital production symposium* (2017), pp. 1–5. 6
- [JYF\*19] JING Y., YANG Y., FENG Z., YE J., YU Y., SONG M.: Neural style transfer: A review. *IEEE transactions on visualization and computer graphics* 26, 11 (2019), 3365–3385. 2
- [kag16] Painter by numbers, 2016. URL: <https://www.kaggle.com/c/painter-by-numbers>. 17
- [KAGS19] KIM B., AZEVEDO V. C., GROSS M., SOLENTHALER B.: Transport-based neural style transfer for smoke simulations. *ACM Transactions on Graphics (TOG)* 38, 6 (nov 2019). doi:10.1145/3355089.3356560. 8, 9, 10, 11, 14, 15, 16
- [KAGS20] KIM B., AZEVEDO V. C., GROSS M., SOLENTHALER B.: Lagrangian neural style transfer for fluids. *ACM Transactions on Graphics (TOG)* 39, 4 (2020), 52–1. 8, 9, 11, 15
- [KAOT23] KANYUK P., AZEVEDO V., ORTIZ R., TANG J.: Singed silhouettes and feed forward flames: Volumetric neural style transfer for expressive fire simulation. In *ACM SIGGRAPH 2023 Talks* (2023), pp. 1–2. 2, 11, 20
- [KCWI12] KYPRIANIDIS J. E., COLLOMOSSE J., WANG T., ISENBERG T.: State of the "art": A taxonomy of artistic stylization techniques for images and video. *IEEE transactions on visualization and computer graphics* 19, 5 (2012), 866–885. 6
- [KKLD23] KERBL B., KOPANAS G., LEIMKÜHLER T., DRETTAKIS G.: 3d gaussian splatting for real-time radiance field rendering. *ACM Transactions on Graphics (ToG)* 42, 4 (2023), 1–14. 6, 7
- [KKP\*22] KOLKIN N., KUCERA M., PARIS S., SYKORA D., SHECHTMAN E., SHAKHAROVICH G.: Neural neighbor style transfer. *arXiv e-prints* (2022), arXiv-2203. 12
- [KKY22] KIM G., KWON T., YE J. C.: Diffusionclip: Text-guided diffusion models for robust image manipulation. In *Proceedings of the IEEE/CVF Conference on Computer Vision and Pattern Recognition* (2022), pp. 2426–2435. 3
- [KPZK17] KNAPITSCH A., PARK J., ZHOU Q.-Y., KOLTUN V.: Tanks and temples: Benchmarking large-scale scene reconstruction. *ACM Transactions on Graphics* 36, 4 (2017). 17, 18
- [KUH18] KATO H., USHIKU Y., HARADA T.: Neural 3d mesh renderer. In *Proceedings of the IEEE conference on computer vision and pattern recognition* (2018), pp. 3907–3916. 8, 10
- [KY22] KWON G., YE J. C.: Clipstyler: Image style transfer with a single text condition. In *Proceedings of the IEEE/CVF Conference on Computer Vision and Pattern Recognition* (2022), pp. 18062–18071. 3
- [KZL\*23] KAWAR B., ZADA S., LANG O., TOV O., CHANG H., DEKEL T., MOSSERI I., IRANI M.: Imagic: Text-based real image editing with diffusion models. In *Proceedings of the IEEE/CVF Conference on Computer Vision and Pattern Recognition* (2023), pp. 6007–6017. 5
- [LBK17] LIU M.-Y., BREUEL T., KAUTZ J.: Unsupervised image-to-image translation networks. In *Advances in neural information processing systems* (2017), pp. 700–708. 5
- [LDMG\*17] LIU S., DE MELLO S., GU J., ZHONG G., YANG M.-H., KAUTZ J.: Learning affinity via spatial propagation networks. *Advances in Neural Information Processing Systems* 30 (2017). 17
- [LE22] LÜDDECKE T., ECKER A.: Image segmentation using text and image prompts. In *Proceedings of the IEEE/CVF Conference on Computer Vision and Pattern Recognition* (2022), pp. 7086–7096. 13, 16
- [LFM\*19] LIU Y., FAN B., MENG G., LU J., XIANG S., PAN C.: Densepoint: Learning densely contextual representation for efficient point cloud processing. In *Proceedings of the IEEE/CVF international conference on computer vision* (2019), pp. 5239–5248. 11
- [LFY\*17] LI Y., FANG C., YANG J., WANG Z., LU X., YANG M.-H.: Universal style transfer via feature transforms. *Advances in neural information processing systems* 30 (2017). 4, 12

- [LGT\*23] LIN C.-H., GAO J., TANG L., TAKIKAWA T., ZENG X., HUANG X., KREIS K., FIDLER S., LIU M.-Y., LIN T.-Y.: Magic3d: High-resolution text-to-3d content creation. In *Proceedings of the IEEE/CVF Conference on Computer Vision and Pattern Recognition* (2023), pp. 300–309. 10
- [LHM\*19] LIU M.-Y., HUANG X., MALLYA A., KARRAS T., AILA T., LEHTINEN J., KAUTZ J.: Few-shot unsupervised image-to-image translation. In *Proceedings of the IEEE International Conference on Computer Vision* (2019), pp. 10551–10560. 5, 17
- [LHW\*18] LAI W.-S., HUANG J.-B., WANG O., SHECHTMAN E., YUMER E., YANG M.-H.: Learning blind video temporal consistency. In *Proceedings of the European conference on computer vision (ECCV)* (2018), pp. 170–185. 17, 18
- [LJX\*23] LI Y., JIANG L., XU L., XIANGLI Y., WANG Z., LIN D., DAI B.: Matrixcity: A large-scale city dataset for city-scale neural rendering and beyond. In *Proceedings of the IEEE/CVF International Conference on Computer Vision* (2023), pp. 3205–3215. 19
- [LLH\*21] LIU S., LIN T., HE D., LI F., WANG M., LI X., SUN Z., LI Q., DING E.: Adaatt: Revisit attention mechanism in arbitrary neural style transfer. In *Proceedings of the IEEE/CVF international conference on computer vision* (2021), pp. 6649–6658. 4
- [LLKY19] LI X., LIU S., KAUTZ J., YANG M.-H.: Learning linear transformations for fast image and video style transfer. In *Proceedings of the IEEE/CVF Conference on Computer Vision and Pattern Recognition* (2019), pp. 3809–3817. 4, 11, 14, 15, 16, 19
- [LLL\*18] LI Y., LIU M.-Y., LI X., YANG M.-H., KAUTZ J.: A closed-form solution to photorealistic image stylization. In *Proceedings of the European Conference on Computer Vision (ECCV)* (2018), pp. 453–468. 4
- [LLLK22] LIAO P., LI X., LIU X., KEUTZER K.: The artbench dataset: Benchmarking generative models with artworks. *arXiv preprint arXiv:2206.11404* (2022). 13
- [LLSH23] LI J., LI D., SAVARESE S., HOI S.: Blip-2: Bootstrapping language-image pre-training with frozen image encoders and large language models. *arXiv preprint arXiv:2301.12597* (2023). 19
- [LMB\*14] LIN T.-Y., MAIRE M., BELONGIE S., HAYS J., PERONA P., RAMANAN D., DOLLÁR P., ZITNICK C. L.: Microsoft coco: Common objects in context. In *European conference on computer vision* (2014), Springer, pp. 740–755. 3, 4, 17
- [LPL\*22] LIU Y., PENG S., LIU L., WANG Q., WANG P., THEOBALT C., ZHOU X., WANG W.: Neural rays for occlusion-aware image-based rendering. In *Proceedings of the IEEE/CVF Conference on Computer Vision and Pattern Recognition* (2022), pp. 7824–7833. 19
- [LPSB17] LUAN F., PARIS S., SHECHTMAN E., BALA K.: Deep photo style transfer. In *Proceedings of the IEEE conference on computer vision and pattern recognition* (2017), pp. 4990–4998. 17
- [LSB\*22] LI Z., SHI J., BI S., ZHU R., SUNKAVALLI K., HAŠAN M., XU Z., RAMAMOORTHI R., CHANDRAKER M.: Physically-based editing of indoor scene lighting from a single image. In *European Conference on Computer Vision* (2022), Springer, pp. 555–572.
- [LTH\*18] LEE H.-Y., TSENG H.-Y., HUANG J.-B., SINGH M., YANG M.-H.: Diverse image-to-image translation via disentangled representations. In *Proceedings of the European conference on computer vision (ECCV)* (2018), pp. 35–51. 5
- [LTI18] LIU H.-T. D., TAO M., JACOBSON A.: Paparazzi: surface editing by way of multi-view image processing. *ACM Transactions on Graphics (TOG)* 37, 6 (2018), 221–1. 1, 8, 9, 10, 14, 15
- [Lum23] LUMA: Luma ai, 2023. URL: <https://lumalabs.ai/>. 1, 20
- [LW16] LI C., WAND M.: Combining markov random fields and convolutional neural networks for image synthesis. In *Proceedings of the IEEE conference on computer vision and pattern recognition* (2016), pp. 2479–2486. 12
- [LXLL23] LI B., XUE K., LIU B., LAI Y.-K.: Bbdm: Image-to-image translation with brownian bridge diffusion models. In *Proceedings of the IEEE/CVF Conference on Computer Vision and Pattern Recognition* (2023), pp. 1952–1961. 5
- [LZC\*23] LIU K., ZHAN F., CHEN Y., ZHANG J., YU Y., SADDIK A. E., LU S., XING E.: Stylerf: Zero-shot 3d style transfer of neural radiance fields. In *Proc. IEEE Conf. on Computer Vision and Pattern Recognition (CVPR)* (2023). 8, 9, 14, 15, 16, 17, 18, 19, 20
- [LZJ\*22] LEI J., ZHANG Y., JIA K., ET AL.: Tango: Text-driven photorealistic and robust 3d stylization via lighting decomposition. *Advances in Neural Information Processing Systems 35* (2022), 30923–30936. 10, 20
- [Man23] MANZANEQUE F. R.: Revolutionizing virtual production: How neural radiance fields will supercharge production pipelines: Neural radiance fields. *Neural Radiance Fields* (Apr 2023). URL: <https://neuralradiancefields.io/>. 2, 20
- [MBBV15] MASCI J., BOSCAINI D., BRONSTEIN M., VANDERGHEYNST P.: Geodesic convolutional neural networks on riemannian manifolds. In *Proceedings of the IEEE international conference on computer vision workshops* (2015), pp. 37–45. 7
- [MBOL\*22] MICHEL O., BAR-ON R., LIU R., BENAÏM S., HANOCKA R.: Text2mesh: Text-driven neural stylization for meshes. In *Proceedings of the IEEE/CVF Conference on Computer Vision and Pattern Recognition* (2022), pp. 13492–13502. 8, 9, 10, 14, 15, 16, 19
- [MBRS\*21] MARTIN-BRUALLA R., RADWAN N., SAJJADI M. S., BARON J. T., DOSOVITSKIY A., DUCKWORTH D.: Nerf in the wild: Neural radiance fields for unconstrained photo collections. In *Proceedings of the IEEE/CVF Conference on Computer Vision and Pattern Recognition* (2021), pp. 7210–7219. 19
- [MESK22] MÜLLER T., EVANS A., SCHIED C., KELLER A.: Instant neural graphics primitives with a multiresolution hash encoding. *ACM Transactions on Graphics (ToG)* 41, 4 (2022), 1–15. 6, 7, 12, 13, 16
- [MHS\*22] MENG C., HE Y., SONG Y., SONG J., WU J., ZHU J.-Y., ERMON S.: SDEdit: Guided image synthesis and editing with stochastic differential equations. In *International Conference on Learning Representations* (2022). 5
- [Mid23] MIDJOURNEY: Midjourney, 2023. URL: <https://www.midjourney.com/>. 1
- [MLS\*22] MENAPACE W., LATHUILLIÈRE S., STAROHIN A., THEOBALT C., TULYAKOV S., GOLYANIK V., RICCI E.: Playable environments: Video manipulation in space and time. In *Proceedings of the IEEE/CVF Conference on Computer Vision and Pattern Recognition* (2022), pp. 3584–3593. 2, 20
- [MOT15] MORDVINTSEV A., OLAH C., TYKA M.: Inceptionism: Going deeper into neural networks. *Google AI Blog* (Jun 2015). Accessed on 18 June 2022. URL: <https://ai.googleblog.com/2015/06/inceptionism-going-deeper-into-neural.html>. 3
- [MPSO18] MORDVINTSEV A., PEZZOTTI N., SCHUBERT L., OLAH C.: Differentiable image parameterizations. *Distill* 3, 7 (2018), e12. 10
- [MRP\*23] METZER G., RICHARDSON E., PATASHNIK O., GIRYES R., COHEN-OR D.: Latent-nerf for shape-guided generation of 3d shapes and textures. In *Proceedings of the IEEE/CVF Conference on Computer Vision and Pattern Recognition* (2023), pp. 12663–12673. 10
- [MSOC\*19] MILDENHALL B., SRINIVASAN P. P., ORTIZ-CAYON R., KALANTARI N. K., RAMAMOORTHI R., NG R., KAR A.: Local light field fusion: Practical view synthesis with prescriptive sampling guidelines. *ACM Transactions on Graphics (TOG)* 38, 4 (2019), 1–14. 17, 18
- [MST\*20] MILDENHALL B., SRINIVASAN P. P., TANCIK M., BARRON J. T., RAMAMOORTHI R., NG R.: Nerf: Representing scenes as neural radiance fields for view synthesis. In *European conference on computer vision* (2020), Springer, pp. 405–421. 6, 7, 8, 12, 13, 14, 16, 17, 18
- [MWLW22] MU F., WANG J., WU Y., LI Y.: 3d photo stylization: Learning to generate stylized novel views from a single image. In *Proceedings of the IEEE/CVF Conference on Computer Vision and Pattern Recognition* (2022), pp. 16273–16282. 11



- [MZS\*23] MA Y., ZHANG X., SUN X., JI J., WANG H., JIANG G., ZHUANG W., JI R.: X-mesh: Towards fast and accurate text-driven 3d stylization via dynamic textual guidance. In *Proceedings of the IEEE/CVF International Conference on Computer Vision (ICCV)* (2023). 1, 8, 9, 10, 15, 16, 17, 19
- [NPLX22] NGUYEN-PHUOC T., LIU F., XIAO L.: Snerf: stylized neural implicit representations for 3d scenes. *ACM Transactions on Graphics (TOG) - Proceedings of ACM SIGGRAPH 2022* (2022). 8, 9, 11, 12, 15, 16, 17, 18
- [NR21] NAVARRO M., RICE J.: Stylizing volumes with neural networks. In *ACM SIGGRAPH 2021 Talks* (2021), pp. 1–2. 2, 6
- [OBW22] ORGHIDAN R., BEDENK T., WEGNER K.: An r&d project on ai for in 3d asset creation for games, 2022. URL: <https://www.endava.com/en/blog/Engineering/2022/An-R-D-Project-on-AI-in-3D-Asset-Creation-for-Games.2>
- [Ope23] OPENAI: Dall-e 3, 2023. URL: <https://openai.com/dall-e-3.1>
- [PEZZ20] PARK T., EFROS A. A., ZHANG R., ZHU J.-Y.: Contrastive learning for unpaired image-to-image translation. In *Computer Vision–ECCV 2020: 16th European Conference, Glasgow, UK, August 23–28, 2020, Proceedings, Part IX 16* (2020), Springer, pp. 319–345. 3, 13
- [PHY23] PANG H.-W., HUA B.-S., YEUNG S.-K.: Locally stylized neural radiance fields. In *Proceedings of the IEEE/CVF International Conference on Computer Vision (ICCV)* (2023). 8, 9, 11, 12, 13, 15, 16
- [PBJM23] POOLE B., JAIN A., BARRON J. T., MILDENHALL B.: Dreamfusion: Text-to-3d using 2d diffusion. In *The Eleventh International Conference on Learning Representations* (2023). 10
- [PKSZ\*23] PARMAR G., KUMAR SINGH K., ZHANG R., LI Y., LU J., ZHU J.-Y.: Zero-shot image-to-image translation. In *ACM SIGGRAPH 2023 Conference Proceedings* (2023), pp. 1–11. 5
- [PL19] PARK D. Y., LEE K. H.: Arbitrary style transfer with style-attentional networks. In *proceedings of the IEEE/CVF conference on computer vision and pattern recognition* (2019), pp. 5880–5888. 4
- [PM11] PHILLIPS F., MACKINTOSH B.: Wiki art gallery, inc.: A case for critical thinking. *Issues in Accounting Education* 26, 3 (2011), 593–608. 4, 11
- [PWS\*21] PATASHNIK O., WU Z., SHECHTMAN E., COHEN-OR D., LISCHINSKI D.: Styleclip: Text-driven manipulation of stylegan imagery. In *Proceedings of the IEEE/CVF International Conference on Computer Vision* (2021), pp. 2085–2094. 3, 13
- [PYG\*23] PO R., YIFAN W., GOLYANIK V., ABERMAN K., BARRON J. T., BERMANO A. H., CHAN E. R., DEKEL T., HOLYNSKI A., KANAZAWA A., LIU C. K., LIU L., MILDENHALL B., NIESSNER M., OMMER B., THEOBALT C., WONKA P., WETZSTEIN G.: State of the art on diffusion models for visual computing. *arXiv 2310.07204* (2023). 5
- [QSMG17] QI C. R., SU H., MO K., GUIBAS L. J.: Pointnet: Deep learning on point sets for 3d classification and segmentation. In *Proceedings of the IEEE conference on computer vision and pattern recognition* (2017), pp. 652–660. 7, 11
- [RBL\*22] ROMBACH R., BLATTMANN A., LORENZ D., ESSER P., OMMER B.: High-resolution image synthesis with latent diffusion models. In *Proceedings of the IEEE/CVF conference on computer vision and pattern recognition* (2022), pp. 10684–10695. 3, 5
- [RDN\*22] RAMESH A., DHARIWAL P., NICHOL A., CHU C., CHEN M.: Hierarchical text-conditional image generation with clip latents. *arXiv preprint arXiv:2204.06125* 1, 2 (2022), 3. 5
- [RK20] RIEGLER G., KOLTUN V.: Free view synthesis. In *European Conference on Computer Vision* (2020), Springer, pp. 623–640. 6, 11, 16
- [RK21] RIEGLER G., KOLTUN V.: Stable view synthesis. In *Proceedings of the IEEE/CVF Conference on Computer Vision and Pattern Recognition* (2021), pp. 12216–12225. 6, 11, 16
- [RKH\*21] RADFORD A., KIM J. W., HALLACY C., RAMESH A., GOH G., AGARWAL S., SASTRY G., ASKELL A., MISHKIN P., CLARK J., ET AL.: Learning transferable visual models from natural language supervision. In *International conference on machine learning* (2021), PMLR, pp. 8748–8763. 3, 5, 16
- [RMA\*23] RICHARDSON E., METZER G., ALALUF Y., GIRYES R., COHEN-OR D.: Texture: Text-guided texturing of 3d shapes. In *ACM SIGGRAPH 2023 Conference Proceedings* (New York, NY, USA, 2023), SIGGRAPH '23, Association for Computing Machinery. doi: 10.1145/3588432.3591503. 1, 8, 9, 10, 14, 15
- [Run23] RUNWAY: Runway, 2023. URL: <https://runwayml.com/1>
- [SBV\*22] SCHUHMAN C., BEAUMONT R., VENCU R., GORDON C., WIGHTMAN R., CHERTI M., COOMBES T., KATTA A., MULLIS C., WORTSMAN M., ET AL.: Laion-5b: An open large-scale dataset for training next generation image-text models. *Advances in Neural Information Processing Systems* 35 (2022), 25278–25294. 5
- [SCC\*22] SAHARIA C., CHAN W., CHANG H., LEE C., HO J., SALIMANS T., FLEET D., NOROUZI M.: Palette: Image-to-image diffusion models. In *ACM SIGGRAPH 2022 Conference Proceedings* (2022), pp. 1–10. 5
- [SCD\*23] SONG H., CHOI S., DO H., LEE C., KIM T.: Blending-nerf: Text-driven localized editing in neural radiance fields. In *Proceedings of the IEEE/CVF International Conference on Computer Vision* (2023). 1, 8, 9, 13, 15, 16
- [SCS\*22] SAHARIA C., CHAN W., SAXENA S., LI L., WHANG J., DENTON E. L., GHASEMIPOUR K., GONTIJO LOPES R., KARAGOL AYAN B., SALIMANS T., ET AL.: Photorealistic text-to-image diffusion models with deep language understanding. *Advances in Neural Information Processing Systems* 35 (2022), 36479–36494. 5
- [SDZ\*21] SRINIVASAN P. P., DENG B., ZHANG X., TANCIK M., MILDENHALL B., BARRON J. T.: Nerv: Neural reflectance and visibility fields for relighting and view synthesis. In *Proceedings of the IEEE/CVF Conference on Computer Vision and Pattern Recognition* (2021), pp. 7495–7504. 20
- [SFHAE23] SELLA E., FIEBELMAN G., HEDMAN P., AVERBUCH-ELOR H.: Vox-e: Text-guided voxel editing of 3d objects. In *Proceedings of the IEEE/CVF International Conference on Computer Vision* (2023), pp. 430–440. 13
- [SGZ\*16] SALIMANS T., GOODFELLOW I., ZAREMBA W., CHEUNG V., RADFORD A., CHEN X.: Improved techniques for training gans. *Advances in neural information processing systems* 29 (2016), 2234–2242. 17
- [SJJ\*21] SINGH A., JAISWAL V., JOSHI G., SANJEEVE A., GITE S., KOTECHA K.: Neural style transfer: A critical review. *IEEE Access* (2021). 2
- [SKH\*23] SHUM K. C., KIM J., HUA B.-S., NGUYEN D. T., YEUNG S.-K.: Language-driven object fusion into neural radiance fields with pose-conditioned dataset updates. *arXiv preprint arXiv:2309.11281* (2023). 13
- [SLJ\*15] SZEGEDY C., LIU W., JIA Y., Sermanet P., REED S., ANGUELOV D., ERHAN D., VANHOUCHE V., RABINOVICH A.: Going deeper with convolutions. In *Proceedings of the IEEE conference on computer vision and pattern recognition* (2015), pp. 1–9. 3
- [SLNG20] SCHWARZ K., LIAO Y., NIEMEYER M., GEIGER A.: Graf: Generative radiance fields for 3d-aware image synthesis. *Advances in Neural Information Processing Systems* 33 (2020), 20154–20166. 14
- [SME21] SONG J., MENG C., ERMON S.: Denoising diffusion implicit models. In *International Conference on Learning Representations* (2021). 5
- [SSC22] SUN C., SUN M., CHEN H.-T.: Direct voxel grid optimization: Super-fast convergence for radiance fields reconstruction. In *Proceedings of the IEEE/CVF Conference on Computer Vision and Pattern Recognition* (2022), pp. 5459–5469. 6, 7, 14, 16



- [SSME23] SU X., SONG J., MENG C., ERMON S.: Dual diffusion implicit bridges for image-to-image translation. In *The Eleventh International Conference on Learning Representations* (2023). 5
- [SVB\*21] SCHUHMANN C., VENCU R., BEAUMONT R., KACZMARCZYK R., MULLIS C., KATTA A., COOMBES T., JITSEV J., KOMATSUZAKI A.: Laion-400m: Open dataset of clip-filtered 400 million image-text pairs. *Data Centric AI NeurIPS Workshop* (2021). 5
- [SVI\*16] SZEGEDY C., VANHOUCHE V., IOFFE S., SHELLEN J., WOJNA Z.: Rethinking the inception architecture for computer vision. In *Proceedings of the IEEE conference on computer vision and pattern recognition* (2016), pp. 2818–2826. 11
- [SVKK\*11] SIDI O., VAN KAICK O., KLEIMAN Y., ZHANG H., COHENOR D.: Unsupervised co-segmentation of a set of shapes via descriptor-space spectral clustering. In *Proceedings of the 2011 SIGGRAPH Asia Conference* (2011), pp. 1–10. 17
- [SWB21] SASAKI H., WILLCOCKS C. G., BRECKON T. P.: Unit-ddpm: Unpaired image translation with denoising diffusion probabilistic models. *arXiv preprint arXiv:2104.05358* (2021). 5
- [SWM\*19] STRAUB J., WHELAN T., MA L., CHEN Y., WIJMAN E., GREEN S., ENGEL J. J., MUR-ARTAL R., REN C., VERMA S., ET AL.: The replica dataset: A digital replica of indoor spaces. *arXiv preprint arXiv:1906.05797* (2019). 19
- [SZ15] SIMONYAN K., ZISSERMAN A.: Very deep convolutional networks for large-scale image recognition. In *International Conference on Learning Representations* (2015). 2
- [Tan19] TANIGUCHI D.: Neural ar: immersive augmented reality with real-time neural style transfer. In *ACM SIGGRAPH 2019 Virtual, Augmented, and Mixed Reality* (2019), pp. 1–1. 2, 6
- [TBTBD22] TUMANYAN N., BAR-TAL O., BAGON S., DEKEL T.: Splicing vit features for semantic appearance transfer. In *Proceedings of the IEEE/CVF Conference on Computer Vision and Pattern Recognition* (2022), pp. 10748–10757. 16
- [TCY\*22] TANCİK M., CASSER V., YAN X., PRADHAN S., MILDENHALL B., SRINIVASAN P. P., BARRON J. T., KRETZSCHMAR H.: Blocknerf: Scalable large scene neural view synthesis. In *Proceedings of the IEEE/CVF Conference on Computer Vision and Pattern Recognition* (2022), pp. 8248–8258. 19
- [TD20] TEED Z., DENG J.: Raft: Recurrent all-pairs field transforms for optical flow. In *Computer Vision—ECCV 2020: 16th European Conference, Glasgow, UK, August 23–28, 2020, Proceedings, Part II 16* (2020), Springer, pp. 402–419. 18
- [THC\*22] TSENG K.-W., HUANG J.-Y., CHEN Y.-S., CHEN C.-S., HUNG Y.-P.: Pseudo-3d scene modeling for virtual reality using stylized novel view synthesis. In *ACM SIGGRAPH 2022 Posters* (July 2022). 2, 6, 11
- [TLC22] TSENG K.-W., LEE Y.-C., CHEN C.-S.: Artistic style novel view synthesis based on a single image. In *Proceedings of the IEEE/CVF Conference on Computer Vision and Pattern Recognition (CVPR) Workshops* (June 2022). 11
- [TSM\*20] TANCİK M., SRINIVASAN P., MILDENHALL B., FRIDOVICH-KEIL S., RAGHAVAN N., SINGHAL U., RAMAMOORTHY R., BARRON J., NG R.: Fourier features let networks learn high frequency functions in low dimensional domains. *Advances in Neural Information Processing Systems* 33 (2020), 7537–7547. 7
- [TTM\*22] TEWARI A., THIES J., MILDENHALL B., SRINIVASAN P., TRETSCHK E., YIFAN W., LASSNER C., SITZMANN V., MARTIN-BRUALLA R., LOMBARDI S., ET AL.: Advances in neural rendering. In *Computer Graphics Forum* (2022), Wiley Online Library, pp. 703–735. 2
- [tur23] Turbosquid, 2023. URL: <https://www.turbosquid.com/>. 17
- [TWN\*23] TANCİK M., WEBER E., NG E., LI R., YI B., WANG T., KRISTOFFERSEN A., AUSTIN J., SALAHİ K., AHUJA A., ET AL.: Nerfstudio: A modular framework for neural radiance field development. In *ACM SIGGRAPH 2023 Conference Proceedings* (2023), pp. 1–12. 16
- [TZFR23] TURKI H., ZHANG J. Y., FERRONI F., RAMANAN D.: Suds: Scalable urban dynamic scenes. In *Proceedings of the IEEE/CVF Conference on Computer Vision and Pattern Recognition* (2023), pp. 12375–12385. 19
- [UNY\*23] UY M. A., NAKAYAMA G. K., YANG G., THOMAS R. K., GUIBAS L., LI K.: Nerf revisited: Fixing quadrature instability in volume rendering. In *Advances in Neural Information Processing Systems (NeurIPS)* (2023). 7
- [UVL16] ULYANOV D., VEDALDI A., LEMPITSKY V.: Instance normalization: The missing ingredient for fast stylization. *arXiv preprint arXiv:1607.08022* (2016). 3
- [Vol23] VOLINGA: Volinga, 2023. URL: <https://volinga.ai/>. 20
- [WCF\*23] WANG Y., CHENG J.-S., FENG Q., TAO W.-Y., LAI Y.-K., LI K.: Tsnerf: Text-driven stylized neural radiance fields via semantic contrastive learning. *Computers & Graphics* 116 (2023), 102–114. 1, 8, 9, 13, 15, 16, 17, 19
- [WCH\*22] WANG C., CHAI M., HE M., CHEN D., LIAO J.: Clip-nerf: Text-and-image driven manipulation of neural radiance fields. In *Proceedings of the IEEE/CVF Conference on Computer Vision and Pattern Recognition* (2022), pp. 3835–3844. 9, 13
- [WDL\*23] WANG H., DU X., LI J., YEH R. A., SHAKHAROVICH G.: Score jacobian chaining: Lifting pretrained 2d diffusion models for 3d generation. In *Proceedings of the IEEE/CVF Conference on Computer Vision and Pattern Recognition* (2023), pp. 12619–12629. 10
- [WGSJ20] WILES O., GKIOXARI G., SZELISKI R., JOHNSON J.: Synsin: End-to-end view synthesis from a single image. In *Proceedings of the IEEE/CVF Conference on Computer Vision and Pattern Recognition* (2020), pp. 7467–7477. 11
- [WJC\*23] WANG C., JIANG R., CHAI M., HE M., CHEN D., LIAO J.: Nerf-art: Text-driven neural radiance fields stylization. *IEEE Transactions on Visualization and Computer Graphics* (2023). 8, 9, 12, 13, 16, 18
- [WLV21] WANG P., LI Y., VASCONCELOS N.: Rethinking and improving the robustness of image style transfer. In *Proceedings of the IEEE/CVF Conference on Computer Vision and Pattern Recognition* (2021), pp. 124–133. 3
- [WLW\*23] WANG Z., LU C., WANG Y., BAO F., LI C., SU H., ZHU J.: Prolificdreamer: High-fidelity and diverse text-to-3d generation with variational score distillation. *Advances in Neural Information Processing Systems* (2023). 10
- [WSK\*15] WU Z., SONG S., KHOSLA A., YU F., ZHANG L., TANG X., XIAO J.: 3d shapenets: A deep representation for volumetric shapes. In *Proceedings of the IEEE conference on computer vision and pattern recognition* (2015), pp. 1912–1920. 7, 17
- [WWG\*21] WANG Q., WANG Z., GENOVA K., SRINIVASAN P. P., ZHOU H., BARRON J. T., MARTIN-BRUALLA R., SNAVELY N., FUNKHOUSER T.: Ibrnet: Learning multi-view image-based rendering. In *Proceedings of the IEEE/CVF Conference on Computer Vision and Pattern Recognition* (2021), pp. 4690–4699. 19
- [WXZ\*20] WANG W., XU J., ZHANG L., WANG Y., LIU J.: Consistent video style transfer via compound regularization. In *Proceedings of the AAAI conference on artificial intelligence* (2020), pp. 12233–12240. 18
- [WYXL20] WANG W., YANG S., XU J., LIU J.: Consistent video style transfer via relaxation and regularization. *IEEE Transactions on Image Processing* 29 (2020), 9125–9139. 18
- [WZDB22] WU Z., ZHU Z., DU J., BAI X.: Ccpl: contrastive coherence preserving loss for versatile style transfer. In *European Conference on Computer Vision* (2022), Springer, pp. 189–206. 13, 17, 18
- [XTS\*22] XIE Y., TAKIKAWA T., SAITO S., LITANY O., YAN S., KHAN N., TOMBARI F., TOMPKIN J., SITZMANN V., SRIDHAR S.: Neural fields in visual computing and beyond. In *Computer Graphics Forum* (2022), Wiley Online Library, pp. 641–676. 2, 7
- [XWC\*23] XU J., WANG X., CHENG W., CAO Y.-P., SHAN Y., QIE X., GAO S.: Dream3d: Zero-shot text-to-3d synthesis using 3d shape prior

- and text-to-image diffusion models. In *Proceedings of the IEEE/CVF Conference on Computer Vision and Pattern Recognition* (2023), pp. 20908–20918. [10](#)
- [XXP\*22] XIANGLI Y., XU L., PAN X., ZHAO N., RAO A., THEOBALT C., DAI B., LIN D.: Bungeenerf: Progressive neural radiance field for extreme multi-scale scene rendering. In *European conference on computer vision* (2022), Springer, pp. 106–122. [19](#)
- [XXP\*23] XU L., XIANGLI Y., PENG S., PAN X., ZHAO N., THEOBALT C., DAI B., LIN D.: Grid-guided neural radiance fields for large urban scenes. In *Proceedings of the IEEE/CVF Conference on Computer Vision and Pattern Recognition* (2023), pp. 8296–8306. [19](#)
- [YGKL21] YARIV L., GU J., KASTEN Y., LIPMAN Y.: Volume rendering of neural implicit surfaces. *Advances in Neural Information Processing Systems* 34 (2021), 4805–4815. [13](#), [16](#)
- [YHY23] YANG S., HWANG H., YE J. C.: Zero-shot contrastive loss for text-guided diffusion image style transfer. In *Proceedings of the IEEE/CVF International Conference on Computer Vision* (2023). [3](#)
- [YKC\*16] YI L., KIM V. G., CEYLAN D., SHEN I.-C., YAN M., SU H., LU C., HUANG Q., SHEFFER A., GUIBAS L.: A scalable active framework for region annotation in 3d shape collections. *ACM Transactions on Graphics (ToG)* 35, 6 (2016), 1–12. [17](#)
- [YUC\*19] YOO J., UH Y., CHUN S., KANG B., HA J.-W.: Photorealistic style transfer via wavelet transforms. In *Proceedings of the IEEE/CVF International Conference on Computer Vision* (2019), pp. 9036–9045. [13](#), [17](#)
- [YZS\*23] YANG L., ZHANG Z., SONG Y., HONG S., XU R., ZHAO Y., ZHANG W., CUI B., YANG M.-H.: Diffusion models: A comprehensive survey of methods and applications. *ACM Computing Surveys* (2023). [5](#)
- [ZH\*23] ZHANG Y., HE Z., XING J., YAO X., JIA J.: Ref-npr: Reference-based non-photorealistic radiance fields for controllable scene stylization. In *Proceedings of the IEEE/CVF Conference on Computer Vision and Pattern Recognition* (2023), pp. 4242–4251. [1](#), [8](#), [9](#), [11](#), [12](#), [15](#), [16](#), [17](#), [18](#), [19](#)
- [ZIE\*18] ZHANG R., ISOLA P., EFROS A. A., SHECHTMAN E., WANG O.: The unreasonable effectiveness of deep features as a perceptual metric. In *Proceedings of the IEEE conference on computer vision and pattern recognition* (2018), pp. 586–595. [16](#)
- [ZJ16] ZHOU Q., JACOBSON A.: Thingi10k: A dataset of 10,000 3d-printing models. *arXiv preprint arXiv:1605.04797* (2016). [17](#)
- [ZJJ\*21] ZHAO H., JIANG L., JIA J., TORR P. H., KOLTUN V.: Point transformer. In *Proceedings of the IEEE/CVF international conference on computer vision* (2021), pp. 16259–16268. [7](#)
- [ZKB\*22] ZHANG K., KOLKIN N., BI S., LUAN F., XU Z., SHECHTMAN E., SNAVELY N.: Arf: Artistic radiance fields. In *European Conference on Computer Vision* (2022), Springer, pp. 717–733. [1](#), [8](#), [9](#), [11](#), [12](#), [13](#), [15](#), [16](#), [18](#), [19](#)
- [ZLH\*23] ZHANG Z., LIU Y., HAN C., PAN Y., GUO T., YAO T.: Transforming radiance field with lipschitz network for photorealistic 3d scene stylization. In *Proceedings of the IEEE/CVF Conference on Computer Vision and Pattern Recognition* (2023), pp. 20712–20721. [8](#), [9](#), [13](#), [15](#), [16](#), [17](#), [18](#)
- [ZPIE17] ZHU J.-Y., PARK T., ISOLA P., EFROS A. A.: Unpaired image-to-image translation using cycle-consistent adversarial networks. In *Proceedings of the IEEE international conference on computer vision* (2017), pp. 2223–2232. [5](#)
- [ZRA23] ZHANG L., RAO A., AGRAWALA M.: Adding conditional control to text-to-image diffusion models. In *Proceedings of the IEEE/CVF International Conference on Computer Vision* (2023), pp. 3836–3847. [5](#), [10](#)
- [ZRSK20] ZHANG K., RIEGLER G., SNAVELY N., KOLTUN V.: Nerf++: Analyzing and improving neural radiance fields. *arXiv preprint arXiv:2010.07492* (2020). [7](#), [14](#), [16](#)
- [ZSD\*21] ZHANG X., SRINIVASAN P. P., DENG B., DEBEVEC P., FREEMAN W. T., BARRON J. T.: Nerfactor: Neural factorization of shape and reflectance under an unknown illumination. *ACM Transactions on Graphics (TOG)* 40, 6 (2021), 1–18. [20](#)
- [ZTD\*22] ZHANG Y., TANG F., DONG W., HUANG H., MA C., LEE T.-Y., XU C.: Domain enhanced arbitrary image style transfer via contrastive learning. *ACM Transactions on Graphics (TOG) - Proceedings of ACM SIGGRAPH 2022* (2022). [4](#)
- [ZWL\*23] ZHUANG J., WANG C., LIU L., LIN L., LI G.: Dreameditor: Text-driven 3d scene editing with neural fields. In *ACM SIGGRAPH Asia 2023 Conference Proceedings* (2023). [13](#)
- [ZYW\*23] ZHAN F., YU Y., WU R., ZHANG J., LU S., LIU L., KORTYLEWSKI A., THEOBALT C., XING E.: Multimodal image synthesis and editing: The generative ai era. In *IEEE Transactions on Pattern Analysis and Machine Intelligence* (2023), IEEE. [2](#), [4](#)